Mineralium Deposita (2020) 55:1625–1646
https://doi.org/10.1007/s00126-020-00990-w

ARTICLE

The Mustajärvi orogenic gold occurrence, Central Lapland Greenstone Belt, Finland: a telluride-dominant mineral system

Matthias Mueller[1,2] · Petri Peltonen[2,3] · Pasi Eilu[4] · Richard Goldfarb[5] · Eero Hanski[1]

Received: 27 June 2019 / Accepted: 17 May 2020 / Published online: 30 June 2020

Abstract

The Mustajärvi gold occurrence lies in the southern part of the Paleoproterozoic Central Lapland Greenstone Belt, in proximity to the first-order transcrustal Venejoki thrust fault system. The gold occurrence is structurally controlled by the second-order Mustajärvi shear zone, which is located at the contact between siliciclastic metasedimentary and mafic to ultramafic metavolcanic rocks. The main mineralization comprises a set of parallel veins and sulfidized rocks that are slightly oblique to the shear zone and are hosted by third-order structures likely representing Riedel R-type shears. The gold-mineralized rock at Mustajärvi is associated with pyrite that is present in 0.15- to 1-m-wide quartz-pyrite-tourmaline veins and in zones of massive pyrite in the host rocks with thicknesses ranging from 1.15 to 2 m. In unweathered rock, hypogene gold is hosted by Au- and Au-Bi-telluride micro-inclusions in pyrite, whereas strong weathering at near surface levels has caused a remobilization of gold, resulting in free gold deposited mainly in the cracks of oxidized pyrite. The geochemistry of both mineralization styles is typical of orogenic gold systems with strong enrichments comprising Au, B, Bi, CO_2, Te, and Se; and less consistent anomalous amounts of Ag, As, Sb, and W. Unusual for orogenic gold deposits is the strong enrichment of Ni and Co, which leads to the classification of Mustajärvi as orogenic gold occurrence with atypical metal association.

Keywords Mustajärvi · Gold · Tellurides · Orogenic gold · Central Lapland Greenstone Belt · Finland

Introduction

The Paleoproterozoic Central Lapland Greenstone Belt (CLGB, Fig. 1) has a total reported gold endowment of just over 10 Moz. Most of this resource is solely defined in the world-class Suurikuusikko deposit, with dozens of other prospective occurrences lacking detailed exploration (Niiranen et al. 2015; Wyche et al. 2015).

One potentially promising target, the Mustajärvi gold occurrence, lies in the southern part of the CLGB, in proximity to the first-order Venejoki thrust fault zone. The Venejoki thrust system has mostly been ignored as a gold exploration target, despite the fact that, regarding the timing and direction of deformation, it is sharing many features with the nearby Sirkka thrust zone which hosts a large proportion of known gold occurrences within the Central Lapland Greenstone Belt (Niiranen et al. 2015). Seismic reflection data indicate the Venejoki fault zone can be traced to the base of the crust at a depth of approximately 42 km (Patison et al. 2006; Niiranen et al. 2014). Few gold occurrences, however, are currently known in proximity to

Editorial handling: F. Molnar

Electronic supplementary material The online version of this article (https://doi.org/10.1007/s00126-020-00990-w) contains supplementary material, which is available to authorized users.

✉ Matthias Mueller
matthiasmueller.geo@gmail.com

[1] Oulu Mining School, University of Oulu, P.O. Box 3000, FI-90014 Oulu, Finland

[2] FireFox Gold Corp., Suite 650, 1021 West Hastings Street, Vancouver, Canada

[3] Department of Geosciences and Geography, Faculty of Science, University of Helsinki, P.O. Box 64, FI-00014 Helsinki, Finland

[4] Geological Survey of Finland, P.O. Box 96, FI-02151 Espoo, Finland

[5] School of Earth Science and Resources, China University of Geosciences (Beijing), Beijing 100083, China

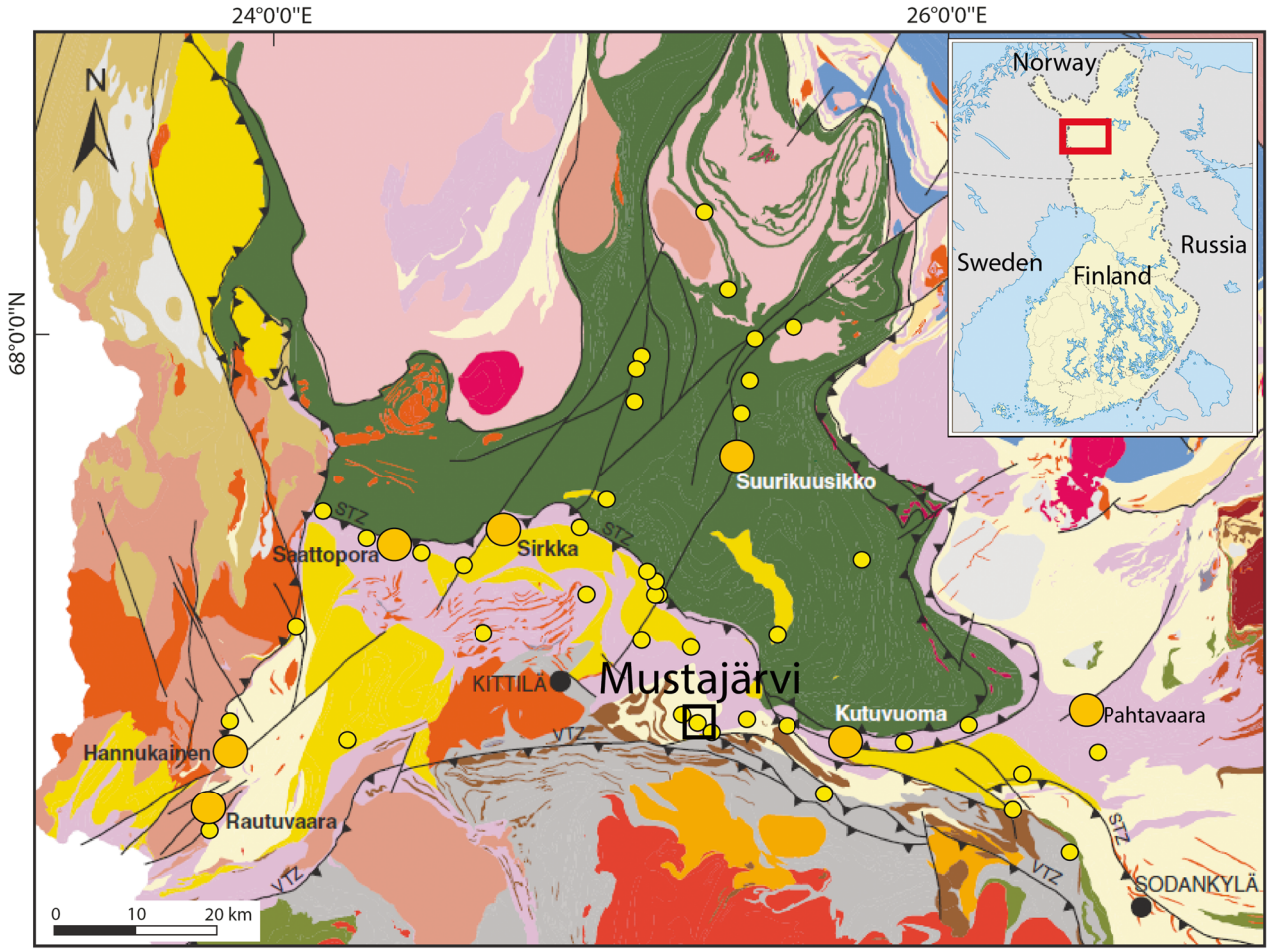

Paleoproterozoic groups

- Kumpu group — Conglomerates, (arkosic) quartzites, minor felsic volcanic rocks
- Kittilä suite — Tholeiitic and minor komatiitic volcanic rocks, graphite- and sulphide-bearing schists, BIFs, phyllites, graywackes
- Savukoski group — Tholeiitic and komatiitic volcanic rocks, phyllites, graphite- and sulphide-bearing schists, tuffites, dolomites
- Sodankylä group — Quartzites, siltstones, mica schists, minor carbonate rocks, mafic volcanic rocks with tuffites
- Kuusamo group — Tholeiitic and minor komatiitic volcanic rocks
- Salla group — Felsic to intermediate volcanic rocks
- Vuojärvi group — Quartzites, mica gneiss, possibly volcanic in origin

Paleoproterozoic complexes

- Lapland granulite complex
- Vuotso complex
- Hetta complex
- Central Lapland Granitoid Complex

Archean complexes

- Pomokaira and Muonio complexes

Paleoproterozoic supracrustal suites

- Nuttio suite
- Olostunturi suite
- Diverse lithodemes

Paleoproterozoic hypabyssal suites

- Haaskalehto gabbro-wehrlite suite

Paleoproterozoic intrusive suites

- Nattanen granite suite
- Haaparanta suite
- Nilipää granite suite
- Eastern Lapland layered intrusion suite
- Keivitsa layered intrusion suite

Major structures

- Shear or fault zone
- Thrust zone

Gold deposits

- Active or past-producing mine
- Prospect

◀ **Fig. 1** Geological map of the CLGB and its known gold occurrences (modified after Eilu and Niiranen 2013). The abbreviations STZ and VTZ, respectively, stand for Sirkka thrust zone and Venejoki thrust zone. The black rectangle around Mustajärvi marks the area of Fig. 2

this deep structure, likely due to the limited exploration activity and the generally poor bedrock exposure.

In this paper, we provide the first overview of the geological setting, structural control, alteration, and style of mineralization of the Mustajärvi occurrence. This represents the first extensively studied gold occurrence along the Venejoki fault system and, significantly, includes necessary background information that should prove helpful in targeting other favorable locations for potential economic gold resources along the structural zone.

Geological setting of the Mustajärvi orogenic gold occurrence

Regional geological setting

The Mustajärvi orogenic gold occurrence is located in the Central Lapland Greenstone Belt in the northern part of the Fennoscandian Shield (Fig. 1). The CLGB of northern Finland is exposed over an area of ~ 100 by 200 km and is part of a larger Paleoproterozoic greenstone system that extends from Russian Karelia in the southeast through Finnish Lapland to northern Norway in the northwest. The CLGB is bordered by the Central Lapland Granitoid Complex to the south and the arc-shaped Lapland Granulite Belt to the northeast. The Paleoproterozoic rocks of the CLGB were deposited on the Archean basement gneisses of the Fennoscandian Shield, beginning at ca. 2.44 Ga (Lehtonen et al. 1998). Approximately 400 million years of prolonged intracratonic to cratonic margin rifting led to accumulation of a sequence of volcanic and sedimentary rocks between 2.44 Ga and 2.0 Ga, which was later multiply deformed during the 1.93–1.77-Ga Svecofennian orogeny (Lehtonen et al. 1998; Hanski and Huhma 2005; Lahtinen et al. 2005; Köykkä et al. 2019). The extensional rifting can be linked globally to the breakup of the Kenorland supercontinent at ca. 2.5–2.1 Ga (Köykkä et al. 2019).

The supracrustal sequence of the CLGB has been divided into six lithostratigraphic groups of metavolcanic and metasedimentary rocks. They comprise, from oldest to youngest, the Salla, Kuusamo, Sodankylä, Savukoski, Kittilä (Kittilä suite), and Kumpu groups (Lehtonen et al. 1998; Hanski and Huhma 2005; Niiranen et al. 2014; Köykkä et al. 2019) (Fig. 1).

The Salla group contains the lowermost units of the CLGB, comprising subaerial calc-alkaline intermediate to felsic metavolcanic rocks, which unconformably overlie the Archean basement in the eastern and northeastern part of the CLGB (Lehtonen et al. 1998; Hanski and Huhma 2005). The 2.44 Ga age for rocks of the Salla group is constrained by mafic-ultramafic layered intrusions (Mutanen and Huhma 2001). Rocks of the Archean basement and the Salla group are overlain by the extensive komatiitic to tholeiitic volcanic rocks of the Kuusamo group. Rocks of both the Salla and Kuusamo groups are thought to represent volcanic activity related to an initial rifting/early syn-rift stage of the Archean basement (Lehtonen et al. 1998; Hanski and Huhma 2005; Köykkä et al. 2019).

Deposition of a thick and widespread, epiclastic sedimentary sequence on top of the older units reflects a subsequent more tranquil tectonic period (Lehtonen et al. 1998; Hanski and Huhma 2005). This sedimentary sequence is represented by the terrestrial to shallow marine orthoquartzites, sericite quartzites, mica schists, and minor carbonate rocks of the Sodankylä group. The prominent abundance of quartzites suggests an extensive widening of the depositional basin from a relatively narrow rift basin after the cessation of Salla and Kuusamo magmatism. A minimum age for the sedimentary sequence of the Sodankylä group is estimated at 2.22 Ga based on dating of crosscutting mafic dikes and sills (Lehtonen et al. 1998; Hanski et al. 2010).

The transition between rocks of the Sodankylä group and the overlying Savukoski group is associated with a deepening of the depositional rift basins (Lehtonen et al. 1998). Thus, the Sodankylä quartzites gradually transition into the phyllite-tuffite-black schist assemblages of the lower Savukoski group, with additional tholeiitic basalts and tuffs. These graphite- and sulfide-bearing, fine-grained sediments may be important sources for S and Au in some orogenic gold occurrences in the CLGB. A minimum age of 2.05 Ga for the rocks of the Savukoski group is provided by dates on intruding layered mafic intrusions and coeval dolerite dikes (Mutanen and Huhma 2001). The upper Savukoski group is characterized by a reactivation of magmatic activity and the filling of the basin with mafic and ultramafic rocks, such as tholeiitic and picritic basalts and komatiites (Lehtonen et al. 1998). These mantle-derived, high-temperature komatiitic and picritic rocks are suggested to represent plume-related volcanism (Hanski et al. 2001) that is coeval with a major rifting event at ca. 2.1 Ga (Perttunen and Vaasjoki 2001; Rastas et al. 2001; Väänänen and Lehtonen 2001; Kyläkoski et al. 2012).

Rocks of the Savukoski group are overlain by those of the Kittilä suite, which is interpreted to have been derived from a complex of island arcs and oceanic plateaus (Hanski and Huhma 2005). The base of the Kittilä suite is defined by a tectonic contact which is thought to represent obduction of the

submarine Kittilä suite rocks onto the older more subaerial autochthonous lithostratigraphic groups of the CLGB at ca. 1.92 Ga (Hanski and Huhma 2005). The lithologies of the Kittilä suite comprise a thick pile of mafic and minor ultramafic metavolcanic rocks with interbeds of greywacke, phyllite, and graphite- and sulfide-bearing schists, and minor carbonate rocks and banded iron formations (Lehtonen et al. 1998). Similar to the sedimentary rocks of the Savukoski group, the deep marine pelitic graphite- and sulfide-bearing units of the Kittilä suite represent favorable sources for metals and sulfur that could be concentrated in epigenetic gold occurrences. Consequently, the Kittilä suite rocks are highly prospective for orogenic gold deposits and host the world-class Suurikuusikko deposit, currently the site of the largest gold mine in Europe (the Kittilä mine) in regards of annual gold production. The age of the rocks of the Kittilä suite is constrained by ca. 2.01 Ga felsic intrusions (Rastas et al. 2001).

Rocks of the Kittilä suite are unconformably overlain by those of the < 1.89 Ga Kumpu group, which is the youngest stratigraphic unit of the CLGB and mainly comprises molasse-like immature clastic sediments, including polymictic conglomerates. The Kumpu group represents a major stratigraphic break, containing detritus from the earlier-formed rocks of the CLGB and was formed during a collisional tectonic stage associated with the Svecofennian orogeny (Hanski and Huhma 2005).

During the 1.93–1.77 Ga Svecofennian orogen, the Paleoproterozoic rocks of the Central Lapland Greenstone Belt were subjected to a complex tectonic evolution comprising several phases of regional ductile deformation followed by brittle orogenic collapse (Ward et al. 1989; Lahtinen et al. 2005, 2012, 2015, 2018; Sayab et al. 2019). A foreland fold-and-thrust belt-type model, with the CLGB being sandwiched between the Central Lapland Granitoid Complex in the south and the Lapland Granulite Belt in the northeast, was proposed by Ward et al. (1989) with N to NE trending dextral shear zones within the CLGB representing reactivated transfer faults (Ward et al. 1989). Further research recognized three main ductile deformation events followed by brittle deformation (Väisänen 2002; Lahtinen et al. 2005; Hölttä et al. 2007; Patison 2007). The first ductile event was caused by the collision between the Norrbotten and Karelia lithospheric blocks between ca. 1.93 and 1.91 Ga, which resulted in an east-vergent thrusting of rocks of the Kittilä suite over and below those of the Savukoski group (Lahtinen et al. 2005; Nironen 2017). This E-W compression generated large-scale folding within the Kittilä suite with N-S striking axial planes and wavelengths of 6–10 km. The second ductile event was caused by the collision between the Lapland-Kola and Karelia lithospheric blocks between 1.90 and 1.89 Ga (Nironen 2017; Lahtinen and Huhma 2019). This resulted in an orthogonal shift in the compression direction from E-W to N-S and caused the northwards thrusting of the Savukoski group over the Kittilä suite along the south-west-dipping, WNW-oriented Sirkka thrust zone, and additional thrusting along the semi-parallel Venejoki thrust zone (Fig. 1) (Hölttä et al. 2007; Patison 2007; Niiranen et al. 2014; Nironen 2017). Furthermore, this N-S shortening resulted in S-SSW directed thrusting of the Lapland Granulite belt onto the CLGB succession rocks (Hölttä et al. 2007; Patison 2007). The timing and nature of the third ductile event is ambiguous, ranging roughly between 1.88 and 1.81 Ga. Recent research divides this event into two individual deformation events (e.g., Nironen 2017; Lahtinen et al. 2018; Sayab et al. 2019). Within this third deformation event, the direction of thrust rotated between NE-SW and NW-SE, creating numerous NE to NNE striking shear zones that are interpreted to be reactivated pre-existing transfer faults (Ward et al. 1989). Due to the rotation of the maximum principal stress, these shear zones are polyphased, with the sense of shear having changed at least once (Patison 2007). The third ductile event furthermore caused a reactivation of the Sirkka and Venejoki fault zones, likely with a strike-slip component (Patison 2007; Nironen 2017). A final deformation event marks the end of the Svecofennian orogeny in the Central Lapland Greenstone Belt and comprises brittle features related to an orogenic collapse between 1.80 and 1.76 Ga (Patison 2007; Nironen 2017). Stephens and Andersson (2015) presented a more continuous accretionary model for the Svecofennian orogeny, based on evidence from the Bergslagen district, Sweden; however, this model does not appear essentially relevant to Central Lapland, Finland. Stephens and Anderssons model was later reworked by Bergman and Weihed (2020). The gold mineralizing events within the CLGB are related to the Svecofennian deformation and coincide with the second Precambrian global peak of orogenic gold mineralization (Goldfarb et al. 2001; Groves et al. 2005). The majority of the gold occurrences in the CLGB formed between 1.80 and 1.76 Ga during the final brittle deformation period and thus orogenic collapse (Patison 2007; Molnar et al. 2017, 2018). However, important ore formation can also be recognized at ca. 1.91 Ga, likely related to the early collision and ductile deformation (Mänttäri 1995; Lahtinen et al. 2012; Molnar et al. 2017, 2018).

Local geology

Mustajärvi lies near the southern border of the CLGB, within 2 km of the transcrustal Venejoki thrust fault (Fig. 1). The local geology at Mustajärvi can be divided into two main units: (1) siliciclastic metasediments consisting of banded

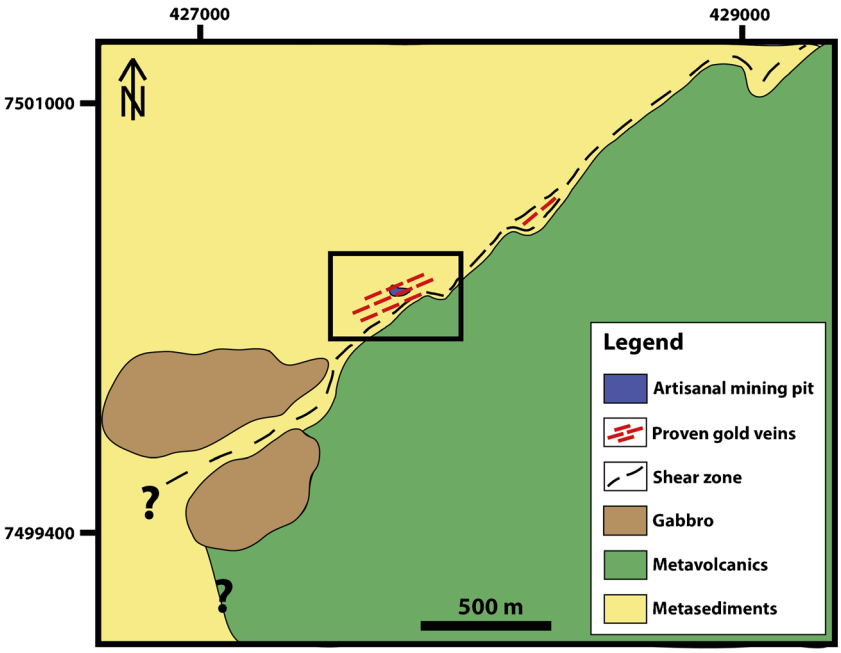

Fig. 2 Simplified geological map of the Mustajärvi study site. The black rectangle marks the extent of the detailed geological map and profile of Fig. 3

arkose quartzites, intermediate tuffites, and mafic tuffites and (2) metavolcanic rocks comprising ultramafic lavas and tuffs, komatiitic basalts, mafic lavas and tuffs, and rare graphitic cherts (Figs. 2 and 3a). The siliciclastic metasediments belong to the Sodankylä group with age estimates of ca. 2.3–2.2 Ga (Lehtonen et al. 1998; Hanski et al. 2010), and the metavolcanic rocks are part of the ca. 2.2–2.06 Ga Savukoski group (Hanski et al. 2001). Both rock units strike roughly northeast with a dip of ~45° to the southeast at Mustajärvi. Gabbroic intrusions of unknown age occur in the southwestern part of the area (Fig. 2).

The main contact between the metasedimentary and metavolcanic rocks, the Mustajärvi shear zone (Figs. 2 and 3), formed due to the rheological differences between the lithologies. The fault, although poorly exposed, is well indicated by features such as a demagnetization, a low apparent resistivity, and a high chargeability in geophysical surveys, and zones of strong deformation and brecciation within drill core observations. Interpretations from the geophysical data and drill core correlations indicate that the fault zone has a similar orientation to the host rocks, dipping towards the southeast at ~50° (Fig. 3b). The siliciclastic metasediments dominantly occur on the northwest side of the fault zone and the metavolcanic rocks dominantly on the southeast side. The contact between the rock units is characterized by an increasing interlayering between the rock types in proximity to the contact zone.

The currently known central gold mineralization consists of three main mineralized veins. The main host is the siliciclastic

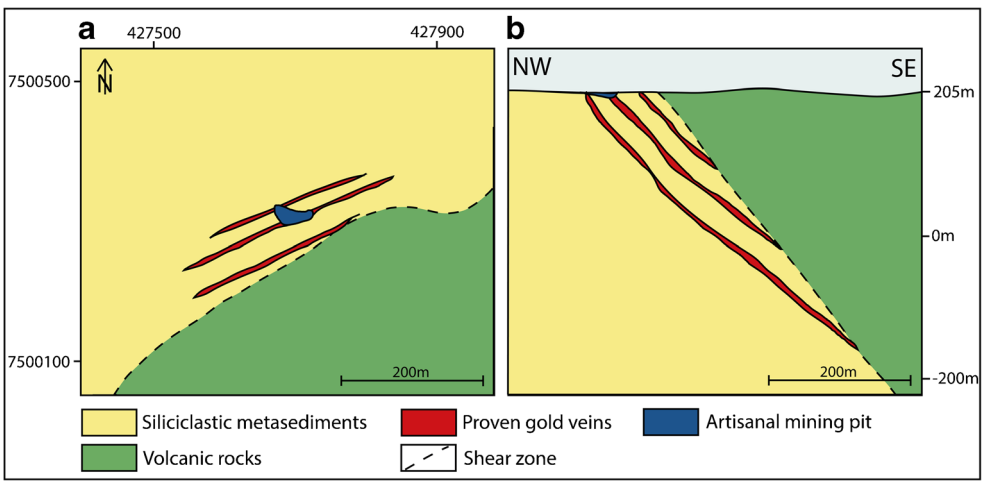

Fig. 3 Detailed geological map (**a**) and geological profile (**b**) of the known central gold mineralization at Mustajärvi. The thickness of the mineralized veins is exaggerated and does not match the scale

metasedimentary rock; however, minor mineralization has also been observed in metavolcanic interlayers in the metasediments, as well as along the contact zones between volcanic interlayers and metasediments. The main mineralization trend has a strike of ~ 065° and is oriented subparallel to the main lithological contact and thus the Mustajärvi shear zone that is striking at ~ 050° (Fig. 3a). At depth, the mineralized veins are slightly offset from the shear zone, at a deviation angle of ~ 5–10° and are thought to be rooted in the fault zone (Fig. 3b).

The currently known extent of the main mineralization is ~ 350 m along strike with proven vertical depths of up to 150 m. In November 2019, substantial new gold mineralization was discovered approximately 600 m northeast of the main mineralized zone (FireFox Gold Corp 2019b), in an interpreted jog of the shear zone (Fig. 2). This suggests a strong structural control of the gold mineralization not solely at the historic Mustajärvi workings but also in prospective sites along the entire shear zone.

Methodology

The Mustajärvi study site, including an artisanal mining pit of ~ 1000 m^2, was mapped in detail and 37 angular boulder and outcrop samples were collected for geochemical analyses and thin section studies. All outcrop samples and most boulder samples originated from within the artisanal pit. Available historic *Outokumpu Oy* drill core was relogged (~ 400 m) and 30 samples from the core were collected for geochemical analyses and thin-section studies. Recent *FireFox Gold Corp* drill core was logged (~2500 m) and geochemical analyses were carried out on selected samples of the core.

A total of 52 thin sections were prepared and studied by transmitted and reflected light microscopy for defining the petrography of the rocks. All presented modal compositions of the rocks are visual estimates based on thin-section studies and drill core observations. A microprobe study with quantitative WDS analysis was subsequently conducted to further investigate the mineralogy of the gold-mineralized rocks. Classification of the gold-related minerals is solely based on their chemical composition measured with quantitative microprobe analysis. All measurements were made at the University of Oulu, utilizing a JEOL JXA-8200 superprobe. The standard operating conditions were 15 kV accelerating voltage with a 15 nA beam current. A tungsten filament was used. The spot size diameter was kept under 1 μm due to the small grain sizes of the gold-associated minerals. Additional measurement parameters, including the peak and background measuring times, the utilized standards, and the data received are given in the electronic supplementary materials (ESMs 1, 4 and 5).

Multi-element geochemical analysis of gold-mineralized drill core samples was performed by *Labtium OY* and consisted of a four-acid digestion with an ICP-MS and ICP-OES finish (code *511PM*). Gold was analyzed using the fire assay method (code *704P*). Additional multi-element geochemical analysis of weathered gold-mineralized samples from outcrop was performed by *ALS Limited* and consisted of a four-acid digestion with an ICP-MS finish (code *ME-MS61*). Gold was analyzed using the fire assay method (code *Au-AA24*). The results from both laboratories included a wide array of elements of interest (ESM 3); however, B, Hg, and Si concentrations were not analyzed.

Petrography of host rock

Siliciclastic metasediments

The siliciclastic metasedimentary rock comprises banded arkose quartzite, intermediate tuffite, and mafic tuffite. In most cases, no clear boundaries between these lithologies can be drawn as the metasedimentary rocks are strongly interlayered on a meter-to-centimeter scale, commonly resulting in a strong banding that is typical of tuffites. The contacts between the individual rock types are mostly gradual. Observed strong banding, felsic clasts in an intermediate to mafic matrix, and local graded bedding suggest a volcaniclastic sedimentation. The entire metasedimentary unit could be described as banded tuffite with variations both in the amount and in geochemistry of volcaniclastic sedimentary input. However, the lack of porphyritic clasts in the arkose quartzites, coupled with the strong albitization and carbonatization, makes the classification of the arkose quartzites as tuffites difficult and hence the general term of siliciclastic metasediments is preferred. Photographs of representative samples of the individual metasedimentary rock types are given in Fig. 4 and an overview of all host rocks and their petrographic features at Mustajärvi is given in ESM 2.

Arkose quartzite makes up the largest part (~ 50 vol%) of the metasedimentary rock package. The color of the rock is generally beige-gray with a pinkish tint (Fig. 4a) due to the common moderate to strong albitization, and occasionally reddish due to silicification with enclosed hematite pigment. Unless strongly altered or brecciated, the rock macroscopically shows primary bedding features including common bands of white mica-rich, grayish-greenish layers (Fig. 4b). Quartz and albite are the main matrix constituents with an average quartz-albite ratio of 60:40. Disseminated carbonate makes up roughly 5–10 vol% of the matrix.

Intermediate tuffite is the second most common rock type in the metasedimentary package, comprising approximately 40 vol% of the unit. The rocks are strongly banded and locally quartz and albitized feldspar clasts resemble pyroclasts in a

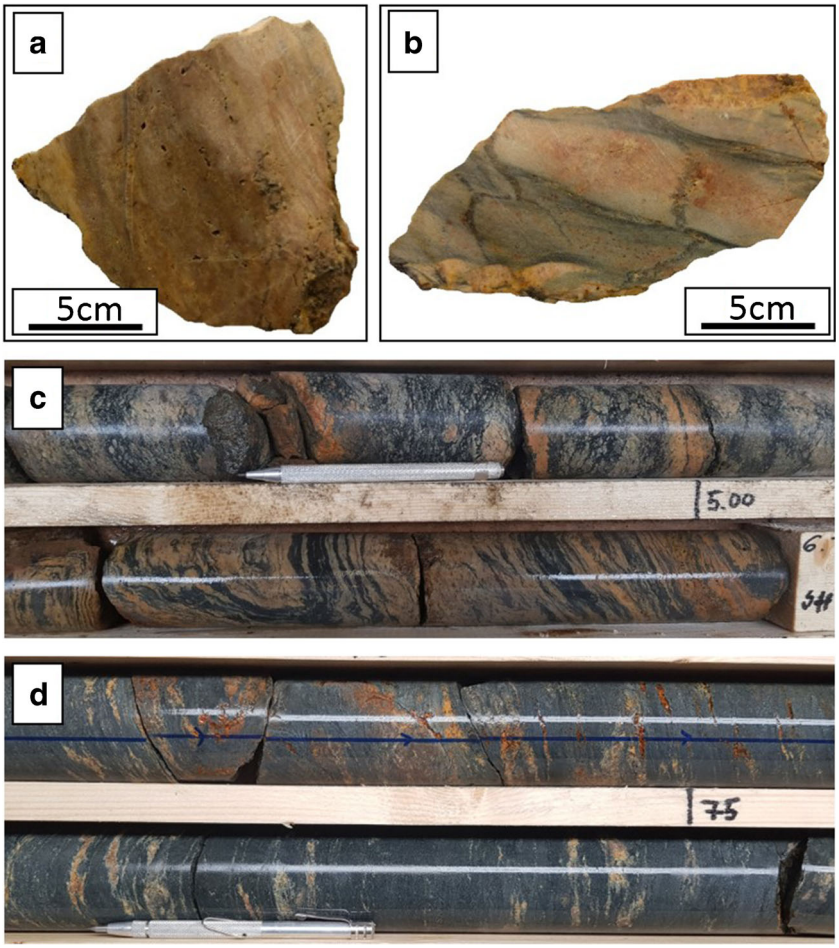

Fig. 4 Representative samples of the metasedimentary rock unit. The drill core diameter is 50.6 mm (NQ2). **a** Strongly albitized arkose quartzite grab sample from the artisanal mining pit. **b** Arkose quartzite grab sample from the artisanal mining pit. The rock displays primary bedding features. **c** Intermediate tuffite. The top row displays porphyritic volcaniclastic sedimentation features with felsic clasts in a mafic matrix. In the bottom row, strongly banded, deformed tuffite with bands of mafic/intermediate and felsic composition. **d** Weakly altered mafic tuffite with concordant quartz-albite-carbonate veining along the foliation

mafic matrix that, together with the graded bedding, suggest a sedimentation influenced by volcanic activity (Fig. 4c). The intermediate tuffite commonly has substantial amounts of biotite; however, in most cases, white mica still dominates over biotite, with its contents being as much as 50 vol% of the rock. Associated with biotite is accessory chlorite, typically in the vicinity of carbonate. Biotite concentrations of > 10 vol% cause the rock to appear dark, making it difficult to macroscopically distinguish between intermediate and mafic tuffite; however, intermediate tuffites are commonly less strongly foliated than mafic tuffites.

Mafic tuffite (Fig. 4c) forms about 10 vol% of the siliciclastic metasedimentary pile. It mostly comprises 0.1- to 1-m thick interlayers, but also rare massive layers with thicknesses of up to 7 m occur. The transition from intermediate tuffite is mostly gradual. The main difference from intermediate tuffite is a higher chlorite and biotite content, which commonly clearly dominates over white mica, and a slightly higher Fe-oxide content. Mafic tuffite can be distinguished from mafic lava by their hardness caused by a higher quartz content and by its moderate foliation due to the layering of quartz with biotite-chlorite bands.

Metavolcanic rocks

The metavolcanic rock unit at Mustajärvi consists of ultramafic lava (komatiite) and tuff, komatiitic basalt, mafic lava (tholeiites) and tuff, and graphitic chert. The different rock types of the volcanic unit are interlayered, with individual layers being 0.1 to 25 m in thickness, thicker layers usually comprising lava and thinner layers being tuff. Photographs of representative samples of the metavolcanic rock types are illustrated in Fig. 5.

The ultramafic lava occurs as massive layers with thicknesses of as much as 25 m. The rock has a pronounced foliation and a dark color with a distinct greenish tint (Fig. 5a). The rock is dominated by fine-grained tremolite and chlorite. With an increasing chlorite and talc content, the rock gains a moderate to strong schistosity and can form distinct talc-chlorite schists in extreme cases. The rock is magnetic, with magnetite occurring both as thin veinlets accompanied by carbonate, and as coarser-grained, more disseminated grains that commonly show chromite remnants in their core.

The ultramafic tuff occurs as 0.1- to 1-m thick interlayers both in (ultra) mafic lavas and siliciclastic metasediments. The

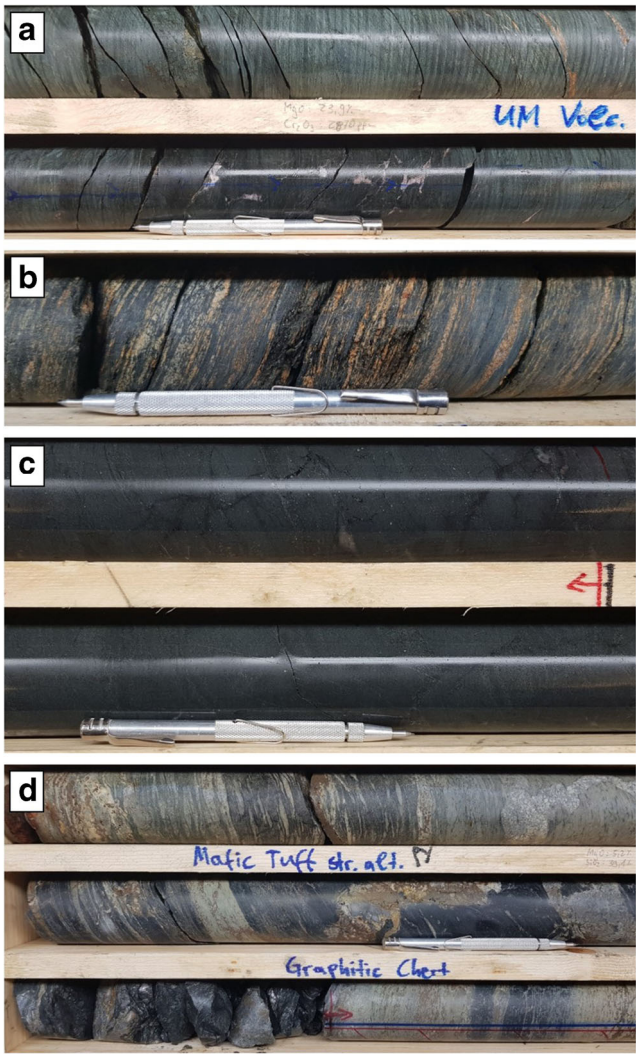

Fig. 5 Representative samples of the metavolcanic rock unit. The drill core diameter is 50.6 mm (NQ2). **a** Massive ultramafic lava. The slightly darker center of the bottom row has a komatiitic basalt geochemical composition. **b** Ultramafic tuff with a strong schistosity and intense parallel quartz-albite-carbonate veining. **c** Least-altered massive mafic lava. **d** Interbedded mafic tuff and graphitic chert that act as zones of strong deformation. The broken rock in the bottom row consists of abundant graphite

tuff has a strong schistosity and is commonly densely veined with quartz-albite-carbonate veins parallel to the schistosity (Fig. 5b). The color of the ultramafic tuff is generally distinctively darker than that of the ultramafic lavas. The rock is commonly non-magnetic to only slightly magnetic.

Komatiitic basalt is the least common rock type of the metavolcanic rock unit. Similar to the ultramafic lava, it occurs as massive layers with a thickness of as much as 15 m. Moreover, it can occur as gradual interlayers in ultramafic lava, whereas the komatiitic basalt does not show the same distinct greenish tint as the ultramafic lava (Fig. 5a). In the komatiitic basalt, actinolite is the dominant amphibole.

Mafic lava of tholeiitic composition occurs as massive units with thicknesses of more than 17 m. Macroscopically, the rock exhibits a massive texture with a weak foliation (Fig. 5c). In most cases, the mafic lava is highly magnetic, which represents an effective tool to distinguish between komatiitic basalts and mafic lavas.

The mafic tuff layers are typically thinner than the lavas and not as massive, with individual layers ranging from 0.1- to 5-m in thickness. The tuffs are tightly banded and consist of a mafic matrix, which is interbedded with lenses or bands of albite and quartz. Mafic tuff layers have been observed to be zones of strong deformation (Fig. 5d). Near the contact zone between siliciclastic metasediments and metavolcanic rocks, altered mafic tuffs occasionally show interbedding with graphitic cherts (Fig. 5d) over an interval of approximately 5–10 m. The graphitic cherts are generally zones of strong deformation and are cut by barren pyrite-rich quartz-albite ± carbonate veins. Graphite occurs in graphite-rich bands with thicknesses of more than 0.3 m.

Alteration

Regional alteration

The degree of regional alteration is generally high in the Sodankylä group metasedimentary rocks and weak to moderate in the Savukoski volcanic rocks (Eilu 1994). At Mustajärvi, regional alteration mainly consists of moderate to strong albitization, mostly in the metasediments; a weak sericitization in the metasediments; and a weak to strong carbonate overprint in both rock units. Furthermore, abundant early-stage quartz-albite veins, commonly with a carbonate overprint, and early-stage carbonate veins occur in both rock units. Albite-rich veins commonly show distinct, bleached, albitization haloes in the metasedimentary rocks.

The regional sodium metasomatism caused the replacement of all feldspars in the metasediments by albite, such that albite makes up 20–60 vol% of the metasedimentary rock. This results in a strong beige to pinkish color of the altered rocks (Fig. 4a). Regional carbonatization is indicated by disseminated carbonate grains, mostly calcite but also lesser dolomite-ankerite, that typically make up 5–10 vol% of the rock mass, based on visual estimates. Furthermore, abundant thin calcite veinlets and semi-massive carbonate veins with both calcite and dolomite-ankerite occur. Carbonate overprints the older albitized rock. Where massive quartz-albite veins also contain carbonate, the latter is best interpreted as an overprinting feature rather than being contemporaneous with the quartz and albite, unless this is a feature of late-orogenic recrystallization. The weak sericitization in the metasediments is mainly represented by a fine-grained sericite growth in the grain boundaries of quartz and albite, but is also observed locally in the core of albite and carbonate grains.

Furthermore, a weak to moderate scapolitization can be locally observed in the siliciclastic metasediments, in places adjacent to veins but more commonly as disseminations.

The metavolcanic rocks are less affected by regional alteration compared to the siliciclastic metasediments. Alteration mostly comprises early-stage quartz-albite veins and abundant carbonate veins. In most cases, quartz-albite veins have accessory sulfide minerals, mainly pyrite, some chalcopyrite, and minor pyrrhotite. Both quartz-albite veins and carbonate veins, primarily consisting of calcite but also of lesser dolomite-ankerite, are mainly concordant with the volcanic rock layers. In contrast to the observed weak regional alteration in the metavolcanic rock, the thin ultramafic tuff layers are generally more strongly altered. They show dense carbonate veining and are locally pervasively altered to biotite. Moreover, rare listvenites were observed as products of intense carbonate + potassic alteration of ultramafic tuff. In most cases, listvenites occur along the contact between ultramafic tuff and siliciclastic metasediment. The listvenites mainly consist of fuchsite cut by intense calcite and dolomite-ankerite veins. Accessory minerals include chlorite, biotite, quartz, albite, rutile, pyrite, and minor chalcopyrite.

Mineralization-related alteration

Mineralization-related alteration in orogenic gold systems can be distinct or more cryptic, and is commonly less developed than in many other hydrothermal mineral deposits (Mikucki and Ridley 1993; Mikucki 1998; Goldfarb et al. 2005). Particularly in clastic metasedimentary host rocks, as in the case of Mustajärvi, such alteration can be subtle due to a low reactivity of the rocks or because unaltered rocks have mineral assemblages largely similar to weakly to moderately altered rock (Bierlein et al. 2004; Goldfarb et al. 2005). Furthermore, the well-developed regional alteration at Mustajärvi makes determination of the gold-related alteration even more difficult. Figure 6 gives a unified overview of the spatial alteration sequences related to ore-forming fluids, which is distinctively different from background alteration and generally applies to most observed mineralized rock at Mustajärvi. Figure 7 shows representative examples of selected mineralization-related alteration features at Mustajärvi.

The most common and nearly ubiquitous mineralization-related alteration is tourmalinization. In the distal alteration

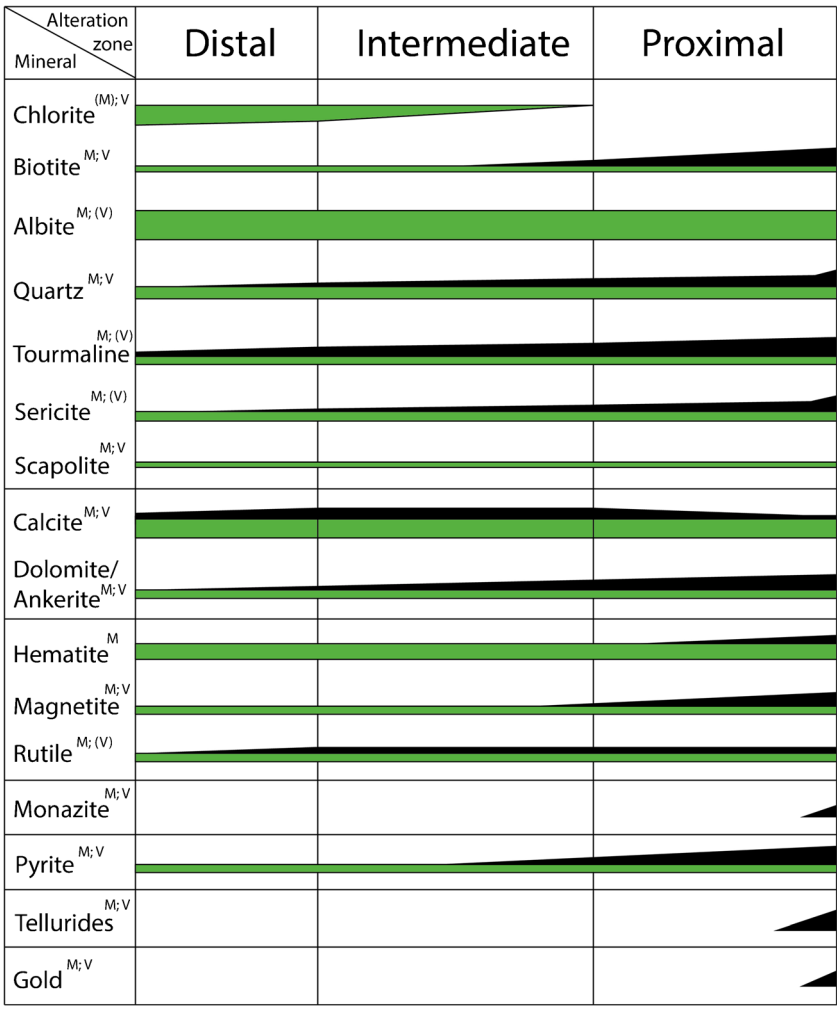

Fig. 6 Schematic overview of the alteration sequence surrounding the gold mineralization at Mustajärvi based on drill core observations and optical microscopy. Letters M and V stand for metasedimentary and metavolcanic rocks, respectively, indicating in which rock unit the alteration occurs. Parentheses indicate a mineral is less common in a unit. Black represents alteration that is most likely related to mineralization and green regional alteration. The proximal, intermediate and distal zones represent distances 0–5 m, 5–25 m, and 25–100 m from the mineralization, respectively

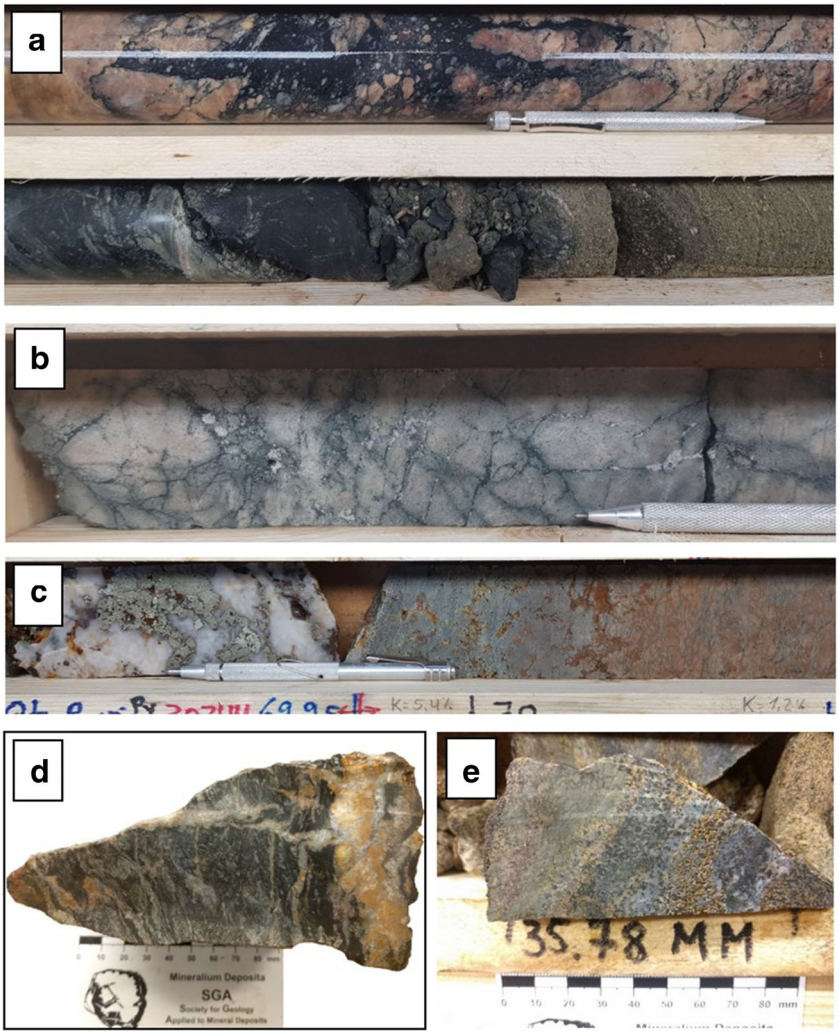

Fig. 7 Representative samples showing selected mineralization-related alteration features. The drill core diameter is 50.6 mm (NQ2). **a** Intense tourmalinization in brecciated metasedimentary rock (top row) and massive tourmaline clusters in totally altered mafic rock with an adjacent pervasively carbonatized zone (bottom row). **b** Biotite stringers in the proximal alteration zone in metasedimentary rock. **c** Narrow proximal alteration zone of strong sericitization adjacent to an auriferous quartz-pyrite-tourmaline vein. **d** Grab sample from the artisanal pit showing a pervasively biotite- and carbonate-altered ultramafic rock. **e** Magnetite-pyrite-carbonate vein in the proximal alteration zone

zone tourmaline occurs as thin veinlets, commonly along quartz-albite ± carbonate vein selvages, or in fractures in the country rock. With decreasing distance to gold-mineralized rock, the tourmaline veining commonly becomes more abundant and locally more massive. In extreme cases, tourmaline forms massive clusters or veins that completely brecciate the host rock (Fig. 7a).

Formation of hydrothermal biotite is also common. In the siliciclastic metasediments, biotite is present in the intermediate alteration zone but is most distinct in the proximal alteration zone. It is commonly observed as thin biotite stringers (Fig. 7b). In the ultramafic volcanic rocks, biotite is pervasively replacing chlorite in the intermediate to proximal alteration zones. It commonly occurs together with extensive carbonate veining. Since this alteration style occasionally also is part of the regional alteration, it is difficult to quantify mineralization-related biotitization within the ultramafic volcanic rocks. Mineralization-related, moderate to intense, sericitization can locally be observed in the proximal alteration zone in the metasediments (Fig. 7c). In contrast, mineralization-related, local fuchsite alteration is noted in the proximal alteration zone in the ultramafic rocks. The fuchsite alteration is strongly linked to carbonate veining. Similar to the biotitization, the sericite and fuchsite are also interpreted to be part of regional alteration, making the identification of gold-related versus regional mica difficult.

The mineralization-related carbonatization is also difficult to distinguish from many areas of local strong regional carbonatization. Nevertheless, commonly, an increase in the density of carbonate veins and vein thickness can be observed with increasing proximity to mineralization, particularly in ultramafic rocks (Fig. 7d). Furthermore, mineralization-related carbonate veins are generally more discordant than carbonate veins related to the regional alteration. Throughout at Mustajärvi, the dominant mineralization-related carbonate phase changes from calcite in the distal to intermediate alteration zone, to dolomite-ankerite in the proximal alteration zone, although some calcite typically remains in the proximal zone too.

In addition to the alteration assemblages given in Fig. 6, the presence of different types of veins indicates proximity to mineralization. Within the intermediate to proximal alteration zone, barren quartz-pyrite ± tourmaline ± carbonate ± albite veins are typical. Locally, gold concentrations are elevated in these veins. Another mineralization indicator is magnetite-pyrite-carbonate veining that, in places, may be present in the proximal alteration zone (Fig. 7e). These veins can be either barren, anomalous in gold, or have high gold concentrations. Also, hematite-pyrite-quartz veins with elevated gold concentrations can be present proximal to mineralization.

Mineralization

Petrography of the gold mineralization

Gold mineralization at Mustajärvi is characterized by pyrite, which can be present in quartz-pyrite-tourmaline veins or as zones of massive pyrite in the host rocks. Representative examples of both mineralization styles are shown in Fig. 8.

The quartz-pyrite-tourmaline veins (Fig. 8a–c) show typical pinch-and-swell features with vein widths ranging between 0.15 and 1 m. Pyrite, the only sulfide mineral in the gold-bearing veins, makes up 5 to 30 vol% of the veins with an average of ~ 10 vol% and has grain sizes ranging between 0.1 and 10 mm, with an average of ~ 2 mm. The amount of tourmaline is very variable, ranging from traces to as much as 35 vol% of the vein. Tourmaline grain sizes range between 20 μm and 1 mm with an average of 0.1 mm. Thin section study of tourmaline-rich parts of the veins reveals a strong textural association and a complex overprinting relationship between pyrite and tourmaline, with pyrite commonly containing abundant euhedral tourmaline inclusions (Fig. 9a–f). The thin-section study, as well as drill core observations, suggest multiple phases of tourmaline crystallization. Accessory minerals in the mineralized veins are white mica and rare monazite (Fig. 9g, h).

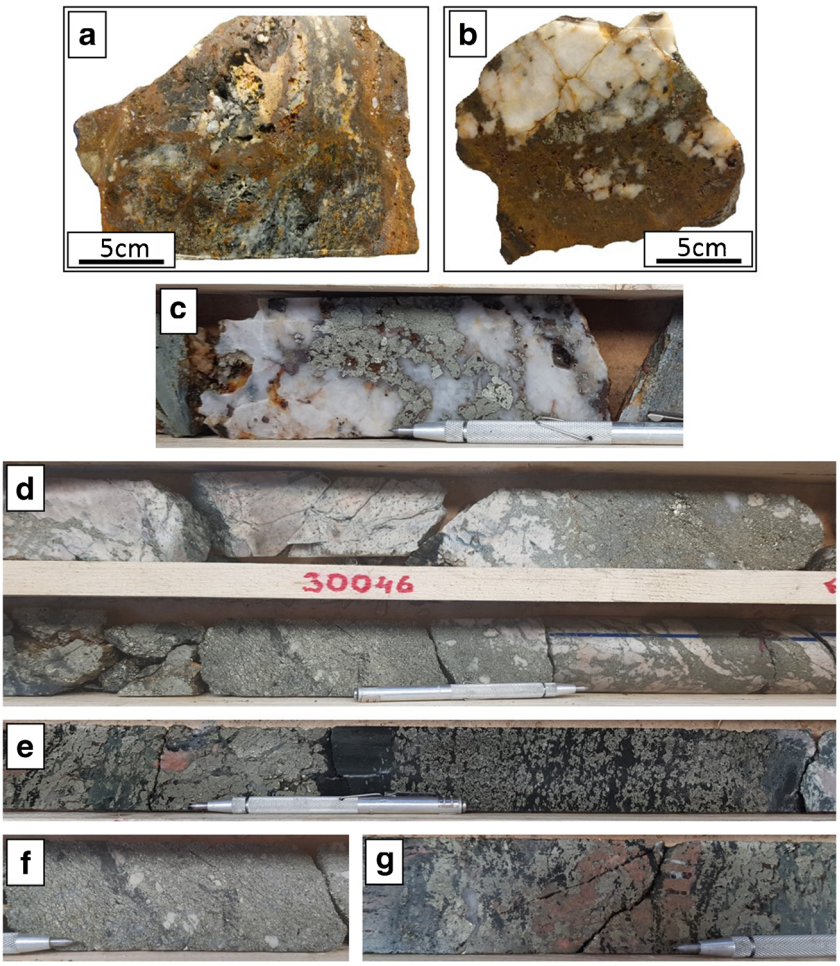

Fig. 8 Examples of the gold mineralization styles at Mustajärvi (**a**–**c** mineralization style 1; **d**–**g** mineralization style 2). The drill core diameter is 50.6 mm (NQ2). **a** Grab sample from the artisanal pit showing an oxidized quartz-pyrite-tourmaline vein with 9.9 ppm Au. **b** Grab sample from the artisanal pit showing a strongly oxidized quartz-pyrite ± tourmaline vein with 63.8 ppm Au. **c** A ~ 15-cm-wide quartz-pyrite-tourmaline vein with 8.4 ppm Au. **d** Parts of a 2-m-wide, highly auriferous, massive pyrite zone in biotite-altered metasedimentary wall rock. This interval contains 2 m of 45.1 ppm Au. **e** Parts of a 1.15-m-wide massive pyrite zone in mainly ultramafic wall rock. The interval contains only 3.8 ppm Au. **f** Close-up view of **d** emphasizing fine-grained anhedral tourmaline amongst pyrite, whereas only accessory quartz is present. **g** Close-up view bordering **e** showing coarse-grained euhedral tourmaline within pyrite

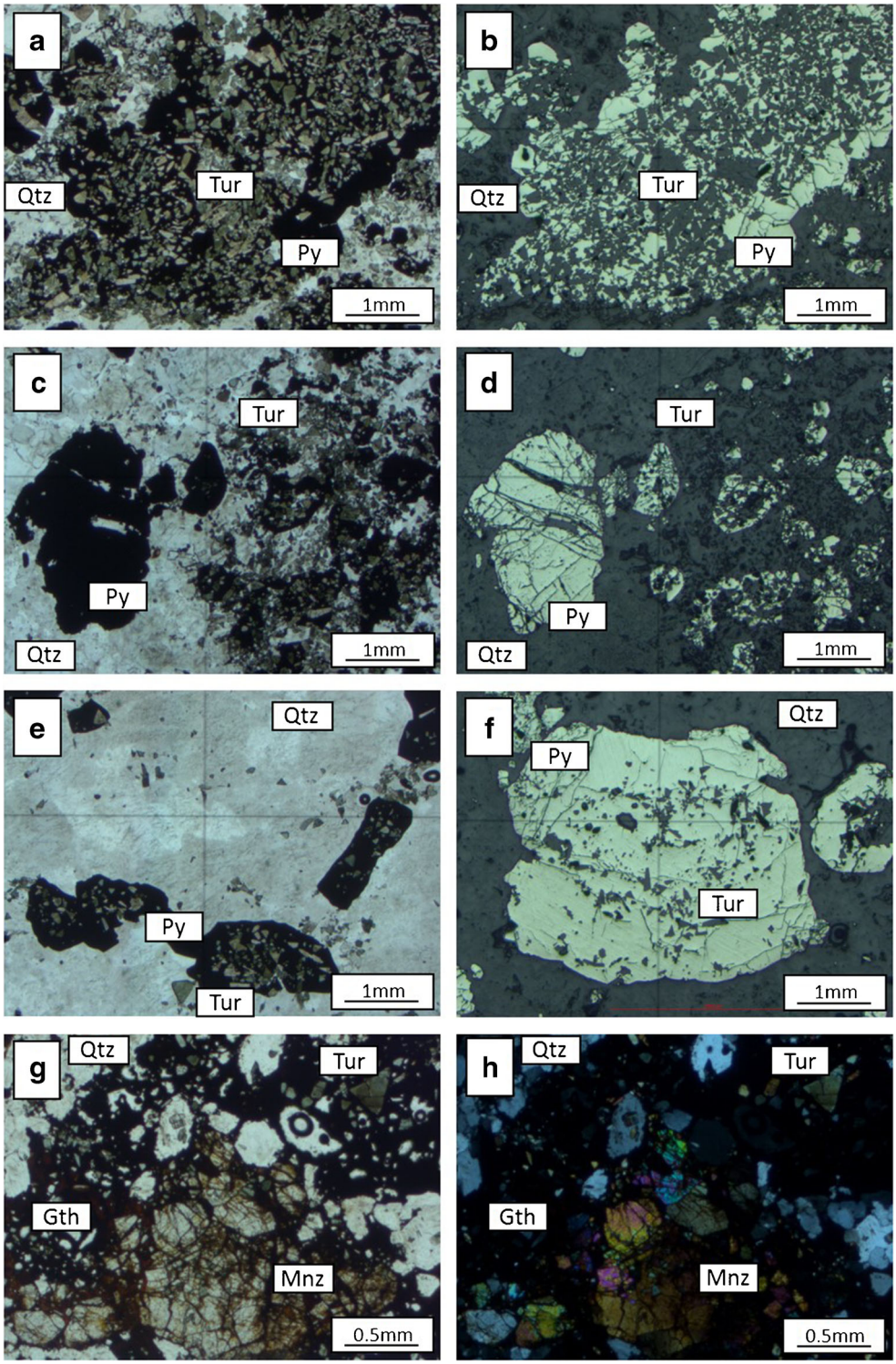

Fig. 9 Photomicrographs of the textural associations and overprinting relationships in unoxidized, tourmaline-rich, mineralized veins. **a**, **b** Abundant tourmaline in a large pyrite grain. **c**, **d** On the right, small pyrite grains show a strong association with tourmaline in contrast to the larger pyrite grain on the left. **e** Tourmaline is commonly located inside or in the vicinity of pyrite. **f** Large pyrite grain with tourmaline inclusions mostly in the center of the grain. **g**, **h** A monazite cluster together with goethite and tourmaline from an oxidized outcropping mineralized vein

Microprobe analyses on samples from outcrop show that gold within the veins is present as Au-telluride (calaverite) and Au-Bi-telluride (montbrayite) micro-inclusions in pyrite (ESM 4). The veins also contain Ni-telluride (melonite), Bi-telluride (tellurobismuthite), and Se-Bi-telluride (kawazulite) (ESM 5). All telluride minerals occur as micro-inclusions in pyrite, with their grain sizes ranging from 1 to 10 μm (Fig. 10). Most telluride minerals form clusters (Fig. 10a) or

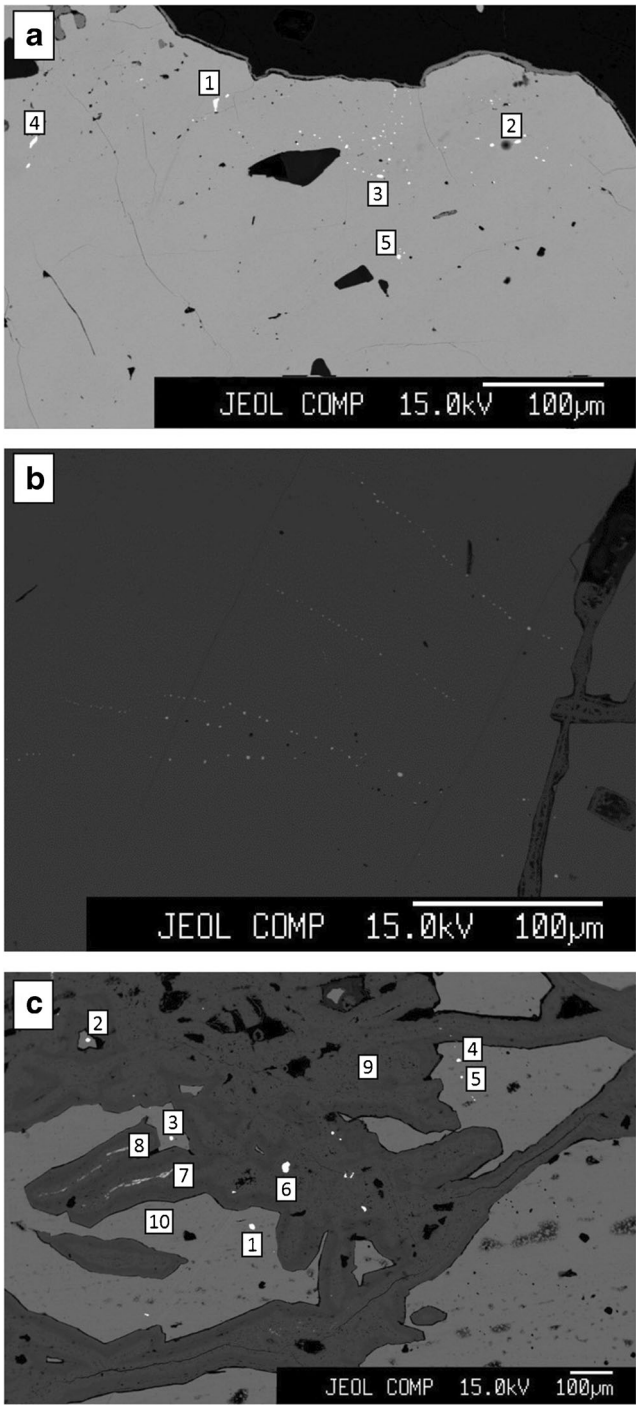

Fig. 10 Back-scattered electron images showing telluride micro-inclusions in pyrite. **a** Melonite (1), montbrayite (2 and 3), kawazulite (4), and calaverite (5) in unoxidized pyrite (gray). **b** Subparallel stringers of montbrayite micro-inclusions (white) in unoxidized pyrite (gray). **c** Pyrite (bright gray: 10) is partly oxidized to goethite (dark gray: 9). Disseminated grains of native Au (white, e.g., 6) in goethite matrix and rare solid solutions of Se-Au-Ag in cracks of goethite (7 and 8). Tellurobismuthite (1), calaverite (3 and 4), and montbrayite (5) in unoxidized pyrite

stringers (Fig. 10b) in pyrite grains, with the exception of melonite that occurs more commonly as single grains disseminated in pyrite and also shows slightly larger grain sizes. No regular spatial relationship, neither between the telluride minerals themselves nor between the tellurides and their location in the host pyrite grain, was observed. In weathered samples, the telluride minerals were destroyed during oxidation of pyrite and Au was locally remobilized and redeposited as native gold near the initial remobilization location (Figs. 10c and 11a–d). Prolonged intense weathering likely further remobilized the native gold, such that much of the gold was observed in cracks in goethite, formed from the breakdown of the pyrite. This dissolution-reprecipitation process during the weathering of hypogene gold-telluride ores is well recognized (e.g., Petersen et al. 1999; Zhao et al. 2009). Free gold has not been observed in unoxidized pyrite at Mustajärvi.

The second mineralization style is characterized by massive pyrite in the metasedimentary and metavolcanic rocks, with mineralized zone widths ranging from 1.15 to 2 m. Pyrite typically makes up between 35 and 60 vol% of the rock. The amount of quartz in the massive pyrite is commonly minor, however, locally quartz veins can be observed on the borders of the massive pyrite. Similar to the vein style of mineralization, the amount of tourmaline varies strongly from trace amounts to 50 vol%. Massive pyrite in metasedimentary rock has yielded the so far highest obtained gold concentrations at Mustajärvi. These include concentrations up to 73.7 ppm Au over 0.5 m in drill core (Fig. 8d, f), with the total mineralized interval yielding 45.1 ppm Au over 2 m (FireFox Gold 2019a). In general, the gold concentrations of the massive pyrite mineralization are rather variable. Thus, although a general positive correlation exists between pyrite volume and gold concentration, it is not a consistent characteristic. For example, one zone of massive pyrite, in ultramafic rock, only yielded 3.8 ppm Au over 1.15 m (Fig. 8e, g). This zone, however, contained very high, distinct, concentrations of approximately 400 ppm Se, while Te and Bi concentrations remained typical for mineralization at Mustajärvi.

Geochemistry of the mineralization

Both vein and massive pyrite mineralization styles show strong enrichment of elements that are commonly elevated in orogenic gold deposits (e.g., Groves et al. 1998; McCuaig and Kerrich 1998; Goldfarb and Groves 2015). At Mustajärvi, these include Au, B, Bi, CO_2, Te, and Se (ESM 3). Other elements that are commonly anomalous in orogenic gold deposits, such as Ag, As, Sb, and W, are elevated at Mustajärvi and have positive correlations with gold but are not enriched to the same extent as the former elements. The Au:Ag ratio at

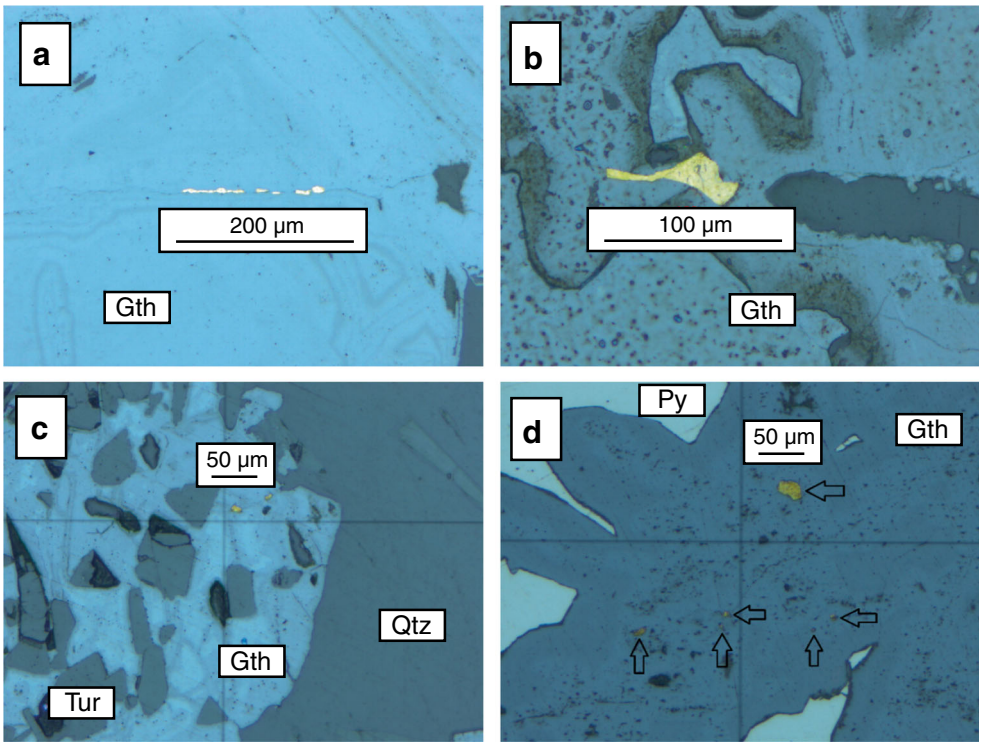

Fig. 11 Reflected light photomicrographs of locally remobilized free gold (yellow) in oxidized pyrite. **a** A stringer of several native gold grains over a length of 200 μm in a crack in goethite. **b** Angular native Au grain in a crack in goethite. **c** Two native gold grains in goethite, which is also enclosing abundant tourmaline grains. **d** One massive and several smaller native gold grains in goethite, adjacent to unoxidized pyrite

Mustajärvi is about 20:1, thus notably higher than the typical ratio of orogenic gold deposits that ranges between 5:1 and 10:1 (Goldfarb et al. 2005). This high ratio is consistent with the lack of silver-bearing tellurides at Mustajärvi. Associated with the generally low As concentrations of gold-bearing samples, neither arsenopyrite nor any other As minerals have been detected at Mustajärvi, and only one arsenian pyrite grain was optically identified in a thin-section sample. Elements that are not commonly elevated in orogenic gold deposits but are clearly enriched at Mustajärvi include Co, Ni, and, to a lesser degree, Mo. Element concentrations of the mineralized rock and selected correlations coefficients are presented as electronic supplementary material (ESM 3); chemical compositions of the Au-bearing minerals and non-auriferous minerals, based on quantitative electron microprobe analysis, are, respectively, also given as electronic supplementary material (ESM 4 and 5).

Tellurium is significantly enriched at Mustajärvi with an average value of ~ 73 ppm in the unweathered mineralized veins (ESM 3). The high Te concentration is related to the abundance of several telluride minerals within pyrite, emphasized by the correlation coefficient of ~ 0.70 between Te and S (ESM 3). The telluride minerals montbrayite and calaverite are the major known gold carriers at Mustajärvi (ESM 4), explaining the strong correlation coefficient of ~ 0.77 between Te and Au. With the oxidation of pyrite during weathering, all telluride minerals are likely destroyed (e.g., Zhao et al. 2009) and tellurium becomes enriched in the resulting goethite (ESM 5).

Bismuth concentrations in the unweathered mineralized veins are significantly enriched with an average of 42.2 ppm. The electron microprobe study indicates that Bi is hosted by micro-inclusions of tellurobismuthite, kawazulite, and montbrayite in pyrite (ESM 4 and 5). This is supported by the correlation coefficients of 0.72 between Bi and S, and 0.75 between Bi and Au. In weathered rock, bismuth is neither hosted in goethite, nor were supergene Bi-bearing phases observed. Yet, the weathered mineralized rocks have an average Bi concentration of 16.7 ppm, suggesting only partial leaching of Bi during weathering. The latter concentration is well above any common unmineralized rock (Rudnick and Gao 2003) leaving it to further studies to determine the Bi-hosting secondary minerals at Mustajärvi.

Selenium concentrations of non-weathered mineralized rocks closely resemble those of Bi, with average and maximum Se contents being 48.6 ppm and 621.0 ppm, respectively. The latter Se level is unusual at Mustajärvi, being associated with an interval within the above-described low-grade massive pyrite intercept, hosted by ultramafic rocks. A noticeable negative correlation between high Se concentrations and low Au concentrations has otherwise not been observed in other mineralized parts at Mustajärvi. Similar to Bi, selenium

is partially leached during weathering, with an average Se concentration of ~ 17 ppm. The electron microprobe study reveals that in non-oxidized mineralized rocks, Se occurs both in kawazulite micro-inclusions in pyrite and in the lattice of pyrite, consistent with the correlation coefficients of 0.71 between Se and Te, and 0.92 between Se and S. In the pyrite lattice, Se constitutes 0.05 wt% of the mineral. Thus, with an average pyrite volume of ~ 10%, in rocks exceeding 0.1 ppm Au, this amounts to ~ 50 ppm Se, suggesting that the lattice of pyrite is the main carrier of Se. In oxidized pyrite, Se was observed to form Se-Au-Ag solid solutions (Fig. 10c), which yielded up to 67.8 wt% Se.

Molybdenum is moderately elevated at Mustajärvi, having an average concentration of 5.3 ppm and a maximum of 104 ppm in unweathered mineralized rock. No Mo-bearing minerals, such as molybdenite, have been observed at Mustajärvi.

Gold in the unweathered mineralized veins has an average concentration of ~ 6.5 ppm and a maximum concentration of 73.7 ppm, based on 35 non-weathered drill core samples exceeding 0.1 ppm Au. As mentioned above, the gold concentration in unweathered veins generally correlates with the pyrite volume; however, notable exceptions exist. The electron microprobe study shows that, the primary gold is hosted in montbrayite and calaverite micro-inclusions within pyrite, which is reflected by the strong correlation of Au with Bi ($\rho = 0.75$) and Te ($\rho = 0.77$). Montbrayite shows a varying chemical composition, with gold concentrations ranging between 8.8 and 46.2 wt%, with an average of 35.0 wt%, and with Au and Bi appearing to substitute for each other (ESM 4). In weathered rock, gold also occurs as native gold, likely formed by destruction of gold-telluride micro-inclusions during the oxidation of pyrite (Figs. 10c and 11a–d). The supergene gold grains are relatively low in silver, with an average of 2.75 wt% Ag. This emphasizes the generally low degree of Ag enrichment, though low silver contents in free gold can also be caused by loss of Ag from the grains during weathering.

Cobalt concentrations in the non-weathered mineralization average 440.6 ppm, with a maximum of 2860 ppm, and with the highest Co concentrations commonly occurring in mineralization hosted in ultramafic rocks. Cobalt is bound in the lattice of pyrite, as suggested by the correlation coefficient between Co and S of 0.94. Electron microprobe analyses yield Co concentrations ranging between 0.12 and 0.76 wt%, with an average of 0.41 wt%, in unoxidized pyrite (ESM 5). No primary cobalt minerals have been observed at Mustajärvi. During oxidation, cobalt is not mobilized, as indicated by an average Co concentration of 0.39 wt% in goethite.

Also nickel is enriched in the auriferous veins at Mustajärvi. In unweathered mineralized rock, Ni has an average value of 114.8 ppm and a maximum of 689 ppm. Electron microprobe analysis shows that nickel occurs in melonite inclusions in pyrite, and in the lattice of pyrite with average concentrations of 0.06 wt%. Therefore, Ni is closely related to the amount of pyrite in the veins, as shown by the correlation coefficient of 0.77 between Ni and S. In weathered rock, Ni is hosted by goethite, which has an average concentration of 0.09 wt% Ni.

Tungsten, uranium, and tin have only been analyzed from weathered rock at Mustajärvi. In samples exceeding 0.1 ppm Au, tungsten is slightly elevated with an average concentration of 1.8 ppm and a maximum of 4.7 ppm. Uranium shows clearly elevated values, with an average concentration of 21.4 ppm and a maximum of 68.2 ppm. Tin is at background levels with an average concentration of 0.3 ppm and a maximum of 0.7 ppm.

Comparisons between unweathered and weathered mineralized rocks show a clear supergene enrichment only for Sb, whereas supergene depletions can be observed in Bi and Se.

Figure 12 compares the Te:Au ratio at Mustajärvi with the published ratios from other orogenic Au and intrusion-related Au deposits. The whole-rock data shows that the average Te:Au ratio of about 11:1 at Mustajärvi is greater than that of the mantle and continental crust and significantly above the average of orogenic and intrusion-related gold deposits, but still within the range of these gold systems. However, it is not yet clear what economic and metallurgic implications, if any, Te-rich gold deposits have. The relationship between tellurium-rich gold deposits and features such as their size, gold grade, formation age, host lithologies, and sulfide volumes are still not well defined and subject of future research (Goldfarb et al. 2017).

Supergene processes

The outcropping mineralized rocks at Mustajärvi have been subject to intense weathering. A schematic profile through the soil and rock package at Mustajärvi is given in ESM 6. The outcropping oxidized mineralized veins and the proximal host rocks are affected by strong clay alteration of albite and micas resulting in the formation of pink and white-beige clay minerals, likely kaolinite. Furthermore, gossan-like, dark-blue-grayish Mn-weathering crusts are present in the intensely clay-altered zones of the artisanal pit (ESM 7a). This weathering crust has only been observed to form on mineralized and non-mineralized quartz veins. Manganese concentrations reach up to 7.3 wt% in these grab samples. No Mn-weathering crusts have observed in any of the drill core.

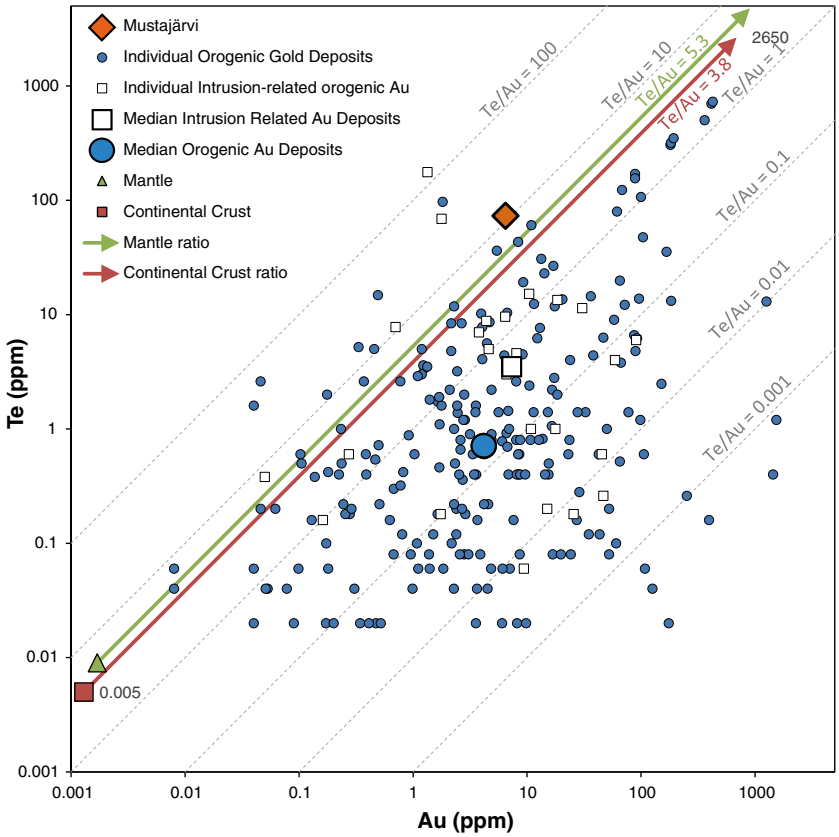

Fig. 12 Diagram showing Te and Au concentrations of multiple orogenic and intrusion-related Au deposits including their median and the Mustajärvi gold deposit. The data from Mustajärvi is based on non-weathered mineralized drill core intercepts exceeding 0.1 ppm in Au (amount of samples: 35; ESM 3). Also shown are average Te/Au ratios of the mantle and continental crust. (modified after Spence-Jones et al. 2018)

Drill hole observations indicate that the intense clay alteration affecting the gold mineralized rock and proximal host rock typically extends from the surface to a depth of at least 25 m. This strong weathering caused core loss of up to 50%, in the mineralized zone during drilling operations. However, not all mineralized veins are clay-altered to the same depth, as some mineralized veins lacking clay alteration were intersected at depths as shallow as about 15 m. Overall, the strong clay alteration is interpreted to be generally 5–25 m deep.

Other supergene effects include the oxidation of pyrite to goethite and the dissolution of carbonates (ESM 7b). The oxidation and weathering of the mineralized rocks causes local supergene enrichments of gold in the clay-altered zone due to an overall loss of rock volume and preferential concentration of gold adsorbed onto secondary minerals. Heavily weathered outcrop samples yield gold concentrations of as much as 140.5 ppm and visible gold is observed. Partial oxidation of the mineralized rock continues below the clay-altered zone, generally down to the depth of ~ 50 m. The intensity and depth of both clay alteration and oxidation are strongly structurally controlled.

Discussion

Structural control

The structural setting at Mustajärvi is typical of that associated with orogenic gold deposits (e.g., Cox 1999; Neumayr et al. 2000; Neumayr and Hagemann 2002; Groves et al. 2003), which involves a first-order structure that focuses and channelizes metal-bearing fluids, and adjacent second-order and possible third-order structures that trap fluids and precipitate the metals. In the case of Mustajärvi, these structures are possibly represented by the transcrustal, first-order, Venejoki thrust fault system that lies ~ 2 km south of Mustajärvi, by the second-order Mustajärvi shear zone, and by the third-order structures that are semi-parallel to the Mustajärvi shear zone and host the gold mineralization (Fig. 3a, b). Being offset by ~ 15° from the shear zone, these third-order structures are interpreted to be Riedel R-type shears (Riedel 1929; Fossen 2010). Formed during prolonged strike-slip movement along the second-order shear zone, these third-order Riedel R-type shears served as suitable traps for the mineralizing fluids. The second-order Mustajärvi shear zone itself displays features of

fault linkage from its early development phases. Based on ground-magnetic data, at least five individual original fault segments can be interpreted (Fig. 2), which were linked during the evolution of the local fault system, forming relay or stepover zones (Fossen 2010). One of these relay zones, approximately 600 m northeast of the main gold mineralization (Fig. 2), is interpreted to have evolved into a structural jog, although it is not evident whether it is a dilational or compressional jog due to the ambiguous shear sense of the fault system. This jog, a suitable structural setting for gold mineralization, was drill-tested and yielded 1.95 m at 12 ppm Au (FireFox Gold Corp 2019b), displaying the strong structural control for mineralization at Mustajärvi.

In proximity to Mustajärvi, the Ahvenjärvi and Lammasvuoma gold occurrences are 2 km to the northwest and 2 km to the southeast of Mustajärvi, respectively (Fig. 1). The gold-mineralized veins at these other two occurrences have the same structural orientation as those at Mustajärvi, striking roughly NE to ENE with a ~ 45° dip to the southeast (Huhtelin 1991; Keinänen 2002; Patison 2007). The same strike direction and the proximity of the Mustajärvi, Ahvenjärvi, and Lammasvuoma gold occurrences suggest a structural connection and an areal extensive gold-forming event.

Alteration

Regional alteration comprises moderate to strong albitization in the siliciclastic metasediments and moderate carbonatization in both the metavolcanic and the metasedimentary packages, which is consistent with observations from many other deposits in the CLGB, e.g., at Saattopora and Suurikuusikko (Eilu 1994; Eilu et al. 2007; Niiranen et al. 2015; Wyche et al. 2015). Pre-mineralization albitized metasediments are typical of many lithological units within the Sodankylä group (Eilu 1994). Eilu (1994) interprets this albitization to be partly related to diagenetic processes, driven by a high-heat flow regime and sea water interaction during a major rifting event. Eilu (1994) finds another cause for albitization and partial carbonatization in the onset of the intrusive activity, regionally creating breccia zones and large hydrothermal cells in the system, triggering alteration. An additional regional, pre-gold alteration event could be related to the Svecofennian orogeny, which caused the formation of large-scale fault zones, such as the Venejoki thrust zone, which represent zones of major fluid flow, perhaps enhanced by associated synorogenic silicic plutonism (Eilu 1994). Auriferous veins at Mustajärvi commonly, but not exclusively, occur in the most intensely albitized parts of the metasediments, and thereby in the most competent rocks, as is common for vein formation in many orogenic gold systems (e.g., Sibson et al. 1988; Cox et al. 1991). We agree with previous findings that albitization was not part of the mineralization-related alteration, particularly because equally intense albitized metasediments can be observed distal to the gold-bearing veins and because pre-gold albitization is ubiquitous at most gold occurrences throughout the CLGB (Eilu 1994; Eilu et al. 2007; Niiranen et al. 2015). Similar early alteration scenarios, with a variable extent, have been suggested also for other Paleoproterozoic supracrustal sequences in the northern Fennoscandian Shield (e.g., Vanhanen 2001; Kyläkoski 2009; Kyläkoski et al. 2012).

The observed mineralization-related alteration features are mostly consistent with those described for orogenic gold deposits globally (Eilu et al. 1999). Yet at Mustajärvi, the mineralization-related alteration is more subtle, and only locally can alteration features be clearly defined. This is consistent with many orogenic gold-related deposits in clastic metasedimentary rocks, which are typically less reactive and more in chemical equilibrium with the hydrothermal fluids and might have pre-gold mineral assemblages partly similar to what is produced by alteration (Bierlein et al. 2004; Goldfarb et al. 2005).

Gold mineralization

Except for the exceptional concentration of the gold seemingly totally in telluride minerals, the gold mineralization features at Mustajärvi are otherwise typical of many orogenic gold systems, including auriferous quartz-pyrite-tourmaline veins with thicknesses ranging between 0.15 and 2.0 m. Pyrite is the only sulfide mineral, suggesting vein formation conditions at $T < 400$ °C and $P < 2.5$ kbar in a hydrothermal environment that was not strongly reduced. On the other hand, occasional biotite in the alteration assemblage suggests a bit higher temperature. Orogenic gold deposits typically have average sulfide mineral amounts of 2–5 vol% (Goldfarb et al. 2005). The average amount of pyrite of 10 vol% at Mustajärvi is not exceptional, however, as many orogenic gold deposits around the world have such a higher sulfide content. At Mustajärvi, gold occurs as gold-bearing telluride microinclusions in pyrite. Gold-telluride systems are commonly considered to result from low-temperature (< 300 °C) processes; however, calaverite has also been reported from moderate- to high-temperature (> 450 °C) deposits (Cabri 1965; Cook et al. 2009). Gold-bearing tellurides in orogenic gold deposits are not uncommon, e.g., in the giant Golden Mile deposit, Western Australia (> 60 Moz mined gold), approximately 20% of the gold is hosted by tellurides (Shackleton et al. 2003), and also in the major Kirkland Lake district in central Canada, a significant part

of the gold resource is in the form of gold-bearing tellurides (Thompson 1949).

It is uncommon for orogenic gold systems to have all gold hosted by tellurides. The large Kensington deposit in Alaska is a rare example where more than 90% of the gold resource is hosted by calaverite (Heinchon 2019), so such examples do exist. The observed textures between tellurides and pyrite, including the occurrence of tellurides as clusters and as sets of parallel stringers in pyrite, possibly indicate a later-stage telluride precipitation in porous pyrite and in micro-fractures of pyrite. Telluride minerals can form due to a decrease in temperature or oxygen fugacity. Hence, interaction of subsequent fluid pulses with earlier deposited pyrite grains could lead to changing redox and favorable conditions for gold-telluride deposition in the pyrite grains; the significant volume of pyrite associated with the gold-telluride ore at the Kensington deposit (e.g., Heinchon 2019) would seem to further support such a hypothesis. Significant drops in temperature are uncommon for orogenic gold system, so we would favor a changing redox scenario for post-pyrite telluride precipitation. Alternatively, if gold-telluride and pyrite precipitation were coeval, such could be explained by relationships shown in Cook et al. (2009). They note that at 250 °C, the stability fields of calaverite and pyrite widely overlap at any pH below 9 but only at very low log fO_2 conditions of −35 to −45; native Au would form as a more stable precious metal stage at most typical hydrothermal fluid redox conditions. At this stage of investigations at Mustajärvi, the observations are not yet sufficient to draw definite conclusions about the timing of gold-telluride precipitation relative to pyrite and precipitation mechanisms for the metals.

The observed Au-Bi-Te compound is ambiguous due to the fact that such a compound has not been known to exist (Ciobanu et al. 2005), however, recently, the mineral formula of montbrayite was revised to include Au, Bi, and Te (Hålenius et al. 2018), which lead to the classification of the at Mustajärvi observed Au-Bi-Te compound as montbrayite. Another possible explanation for the observed compound could be a mix of exsolution of calaverite and tellurobismuthite, but no heterogeneities were observed in these mineral grains during electron microprobe studies.

The geochemical signature of the Mustajärvi mineralization is typical of many orogenic gold deposits with strong enrichments in Au, B, Bi, CO_2, Te, and Se (e.g., Groves et al. 1998, McCuaig and Kerrich 1998, Goldfarb and Groves 2015). Other pathfinder elements that are commonly enriched in orogenic gold systems, such as Ag, As, Sb, and W, are only weakly to moderately enriched, but do show a positive correlation with gold. Atypical of most orogenic gold deposits are the enrichments of Co and Ni. Nevertheless, such Co and Ni anomalies have been described for orogenic gold occurrences in the Kuusamo Schist Belt (e.g., Juomasuo), and the Peräpohja Schist Belt (e.g. Rajapalot), and for orogenic gold occurrences along the WNW-oriented transcrustal Sirkka thrust fault within the CLGB (e.g., Levijärvi-Loukinen) (e.g., Pankka and Vanhanen 1992; Holma and Keinänen 2007; Eilu 2015; Ranta et al. 2018). These gold occurrences have been generally classified as orogenic gold with atypical metal association, which in northern Finland are characterized by enrichments in Cu, Co, Ni, and/or U (Vanhanen 2001; Eilu et al. 2007; Eilu 2015). Regarding this classification, it is here proposed that Mustajärvi is an orogenic gold occurrence with atypical metal association. Orogenic gold systems with an atypical metal association may have formed where Paleoproterozoic tectonism included the pre-orogenic deformation of intracratonic basins, mobilizing anomalously saline basinal fluids (e.g., Goldfarb et al. 2001; Yardley and Graham 2002; Yardley and Cleverley 2013). This model is fully consistent with the crustal evolution of the Karelian domain of Finland, including the CLGB, where supracrustal sequences, including evaporites, formed in rift-related intracratonic basins between 2.44 and 2.0 Ga (Lahtinen et al. 2005, 2012; Eilu 2015; Köykkä et al. 2019). Alternatively, the enrichment of Ni at Mustajärvi, which is mainly hosted in pyrite but also occurs as Ni-telluride micro-inclusions in pyrite, could be explained by the high lithogeochemical background of ultramafic rocks in the gold occurrence area. At Mustajärvi, the ultramafic lavas and tuffs have Ni concentrations of as much as 1000 ppm, with averages of ~ 450 ppm Ni. The correlation of elevated Ni in gold mineralization with ultramafic host rocks has been observed in many gold occurrences along the Sirkka thrust fault (e.g., Eilu et al. 2007). However, a sole source of Co from the local host rocks is questionable because average Co concentrations are ~ 50 ppm in ultramafic rocks, ~ 25 ppm in mafic rocks, and ~ 5 ppm in the siliciclastic metasediments at Mustajärvi.

Classifications other than orogenic gold for Mustajärvi are unreasonable. Classification as a Blackbird-type deposit, due to the high Co concentration, as has been proposed for some of the Co-bearing gold occurrences in the Kuusamo Schist Belt (Slack et al. 2010; Slack 2012), is disregarded due to the lack of elevated Cu concentrations and the strong structural, non-stratiform control of the gold at Mustajärvi (e.g., Earhart 1986; Slack 2012). Similarly, the classification of Mustajärvi as reduced intrusion-related gold occurrence is disregarded because of a lack of potential causative intrusions in the area. The only intrusive system that is coeval with the main gold mineralization age of the gold occurrences along

the Sirkka and Venejoki thrust faults is the ~1.8-Ga Nattanen Granite suite (Heilimo et al. 2009; Molnar et al. 2017, 2018). However, the Nattanen granites are only known from the northern but not from the southern part of the CLGB. Furthermore, no regional enrichments in W or Sn or metal zoning surrounding Mustajärvi, as is common for such magmatic-hydrothermal systems (e.g., Thompson et al. 1999; Lang and Baker 2001; Goldfarb et al. 2005), are recognized.

Conclusions

Gold mineralization at Mustajärvi has a strong structural control, being hosted by third-order structures, possibly Riedel R-type shears, that splay off the second-order Mustajärvi shear zone which is likely to have formed due to the competency contrast between the highly albitized siliciclastic metasedimentary and the metavolcanic rocks in the mineralized area. Gold mineralization is associated with pyrite that is present in quartz-pyrite-tourmaline veins with thicknesses ranging between 0.15 and 1 m and in massive pyrite clots in the host rocks with mineralized thicknesses ranging between 1.15 and 2 m. Gold within the studied mineralization occurs as Au-telluride (calaverite) and Au-Bi-telluride (montbrayite) micro-inclusions in pyrite. Other telluride minerals include the Ni-telluride melonite, the Bi-telluride tellurobismuthite, and the Bi–Se-telluride kawazulite. In the upper tens of meters of the occurrence, the pyrite was oxidized during weathering, the telluride micro-inclusions were dissolved, and Au was remobilized and reprecipitated as free gold, mainly in the cracks of goethite. The geochemistry of the mineralized rock is typical of orogenic gold deposits with consistent strong enrichments in Au, B, Bi, CO_2, Te, and Se, and weak to moderate enrichments in Ag, As, Sb, and W. The enrichment of Ni and Co in the mineralized rock further leads to the classification of Mustajärvi as an orogenic gold occurrence with atypical metal association.

Acknowledgments Acknowledgments go to the entire FireFox Gold Corp team for providing an inspiring and constructive work environment, and particularly the continual support of Carl Löfberg. Juhani Ojala and the Geological Survey of Finland (GTK) are thanked for supporting this research and for providing partial funding. Also, the University of Oulu is thanked for providing funding and infrastructure for this study. Tero Niiranen from the GTK is thanked for his continuous support that helped to improve the quality of this work. Jukka-Pekka Ranta and an anonymous reviewer are thanked for their critical reviews of the manuscript.

Funding Information Open access funding provided by University of Oulu including Oulu University Hospital.

References

Bergman S, Weihed P (2020) Archean (>2.6 Ga) and Paleoproterozoic (2.5–1.8 Ga), pre- and syn-orogenic magmatism, sedimentation and mineralization in the Norrbotten and Överkalix lithotectonic units, Svecokarelian orogen. In: Stephens MB, Bergman Weihed J (eds) Sweden: Lithotectonic framework, vol 50. Tectonic Evolution and Mineral Resources. Geological Society, London, pp 21–81. https://doi.org/10.1144/M50-2016-29

Bierlein FP, Arne DC, Cartwright I (2004) Stable isotope (C, O, S) systematics in alteration haloes associated with orogenic gold mineralization in the Victorian gold province, SE Australia. Geochem Expl Env Anal 4:191–211. https://doi.org/10.1144/1467-7873/04-201

Cabri LJ (1965) Phase relations in the Au-Ag-Te system and their mineralogical significance. Econ Geol 60:1569–1605. https://doi.org/10.2113/gsecongeo.60.8.1569

Ciobanu C, Cook N, Pring A (2005) Bismuth tellurides as gold scavengers. In: Mao J, Bierlein F (eds) Mineral deposit research: meeting the global challenge. Springer, Berlin Heidelberg, pp 1383–1386. https://doi.org/10.1007/3-540-27946-6_352

Cook N, Ciobanu C, Spry P, Voudouris P (2009) Understanding gold-(silver)-telluride-(selenide) mineral deposits. Episodes 32:249–263

Cox SF (1999) Deformational controls in the dynamics of fluid flow in mesothermal gold systems. Geol Soc Spec Publ 155:123–140

Cox SF, Wall VJ, Etheridge MA, Potter TF (1991) Deformational and metamorphic processes in the formation of mesothermal vein-hosted gold deposits – examples from the Lachlan Fold Belt in central Victoria, Australia. Ore Geol Rev 6:391–423. https://doi.org/10.1016/0169-1368(91)90038-9

Earhart RL (1986) Descriptive model of blackbird Co-Cu sulfide. U.S. Geol Surv Bull 1693:1–142

Eilu P (1994) Hydrothermal alteration in volcano-sedimentary rocks in the Central Lapland greenstone belt. Finland Geol Surv Finl Bull 374

Eilu P (2015) Overview on gold deposits in Finland. In: Maier WD, Lahtinen R, O'Brien H (eds) Mineral deposits of Finland. Elsevier, Amsterdam, pp 377–403. https://doi.org/10.1016/B978-0-12-410438-9.00015-7

Eilu P, Niiranen T (2013) Gold deposits in northern Finland Geol Surv Swed Excursion Guidebook FIN1

Eilu P, Mathison C, Groves D, Allardyce W (1999) Atlas of alteration assemblages, styles, and zoning in orogenic lode-gold deposits in a variety of host rock and metamorphic settings. Geology and Geophysics Departments (Centre for Strategic Mineral Deposits) & UWA Extension. Univ West Austr Publ 30

Eilu P, Pankka H, Keinänen V, Kortelainen V, Niiranen T, Pulkkinen E (2007) Characteristics of gold mineralization in the greenstone belts of northern Finland. Geol Surv Finl Spec Pap 44:57–106

FireFox Gold Corp (2019a) FireFox gold intersects high-grade gold at Mustajärvi property: 2 Metres @ 45 g/t gold. https://wwwfirefoxgoldcom/indexphp/news/news-2019/125-firefox-gold-intersects-high-grade-gold-at-mustajaervi-property-2-metres-45-g-t-gold Accessed (14 June 2019)

FireFox Gold Corp (2019b) FireFox gold significantly extends mineralization at Mustajärvi gold project. Finland https://wwwfirefoxgoldcom/indexphp/news/news-2019/166-firefox-gold-significantly-extends-mineralization-at-mustajaervi-gold-project-finland Accessed (07 December 2019)

Fossen H (2010) Structural geology. Cambridge University Press, Cambridge. https://doi.org/10.1017/CBO9780511777806

Goldfarb RJ, Groves DI (2015) Orogenic gold: common or evolving fluid and metal sources through time. Lithos 233:2–26. https://doi.org/10.1016/j.lithos.2015.07.011

Goldfarb RJ, Groves DI, Gardoll S (2001) Orogenic gold and geological time: a global synthesis. Ore Geol Rev 18:1–75. https://doi.org/10.1016/S0169-1368(01)00016-6

Goldfarb RJ, Baker T, Dubé B, Groves DI, Hart CJR, Gosselin P (2005) Distribution, character, and genesis of gold deposits in metamorphic terranes. Econ Geol 100th Anniv Vol pp 407–450. https://doi.org/10.5382/AV100.14

Goldfarb R, Berger B, George M, Seal R (2017) Tellurium. In: Schulz K, DeYoung J, Seal R, Bradley D (eds.) Critical mineral resources of the United States—economic and environmental geology and prospects for future supply. U.S. Geol Surv Prof Pap 1802:1–27

Groves DI, Goldfarb RJ, Gebre-Mariam M, Hagemann SG, Robert F (1998) Orogenic gold deposits: a proposed classification in the context of their crustal distribution and relationship to other gold deposit types. Ore Geol Rev 13:7–27. https://doi.org/10.1016/S0169-1368(97)00012-7

Groves DI, Goldfarb RJ, Robert F, Hart CJR (2003) Gold deposits in metamorphic belts: overview of current understanding, outstanding problems, future research, and exploration significance. Econ Geol 98:1–29. https://doi.org/10.2113/gsecongeo.98.1.1

Groves DI, Condie KC, Goldfarb RJ, Hronsky JMA, Vielreicher RM (2005) Secular changes in global tectonic processes and their influence on the temporal distribution of gold-bearing mineral deposits. Econ Geol 100:203–224. https://doi.org/10.2113/gsecongeo.100.2.203

Hålenius U, Hatert F, Pasero M, Mills S (2018) IMA Commission on new minerals, nomenclature and classification (CNMNC) newsletter 41. Eur Jour Min 30:183–186. https://doi.org/10.1127/ejm/2018/0030-2736

Hanski E, Huhma H (2005) Central Lapland greenstone belt. In: Lehtinen M, Nurmi PA, Rämö OT (eds) Precambrian bedrock of Finland—key to the evolution of the Fennoscandian shield. Elsevier, Amsterdam, pp 139–193. https://doi.org/10.1016/S0166-2635(05)80005-2

Hanski E, Huhma H, Rastas P, Kamenetsky VS (2001) The Palaeoproterozoic komatiite-picrite association of Finnish Lapland. J Petrol 42(5):855–876. https://doi.org/10.1093/petrology/42.5.855

Hanski E, Huhma H, Vuollo J (2010) SIMS zircon ages and Nd isotope systematics of the 2.2 Ga mafic intrusions in northern and eastern Finland. Bull Geol Soc Finl 82:31–62

Heilimo E, Jaana Halla J, Lauri LS, Rämö T, Huhma H, Kurhila MI, Front K (2009) The Paleoproterozoic Nattanen-type granites in northern Finland and vicinity – a postcollisional oxidized A-type suite. Bull Geol Soc Finl 81:7–38

Heinchon SH (2019) Metal and mineral zoning and ore paragenesis at the Kensington Au-Te deposit, SE Alaska. University of Alaska Fairbanks, MSc thesis

Holma M, Keinänen V (2007) The Levijärvi-Loukinen gold occurrence: an example of orogenic gold mineralisation with atypical metal association. Geol Surv Finl Spec Pap 44:163–184

Hölttä P, Väisänen M, Väänänen J, Manninen T (2007) Paleoproterozoic metamorphism and deformation in central Finnish Lapland. Geol Surv Finl Spec Pap 44:109–120

Huhtelin T (1991) Lammasvuoman Au-mineralisaation tutkimukset 1989–1991. Lapin Malmi Rep 001/2734/TH/91 **(in Finnish)**

Keinänen V (2002) Tutkimustyöselostus Kittilän kunnassa valtausalueilla Pikku Mustavaara 1 (kaiv.rek.n:o 6512/1) ja Isomaa 1 (kaiv.rek.n:o 5699/1) suoritetuista malmitutkimuksista. Geol Surv Finl Rep M06/2734/2002/2/10 **(in Finnish)**

Köykkä J, Lahtinen R, Huhma H (2019) Provenance evolution of the Paleoproterozoic metasedimentary cover sequences in northern Fennoscandia: age distribution, geochemistry, and zircon morphology. Precambrian Res 331:105364. https://doi.org/10.1016/j.precamres.2019.105364

Kyläkoski M (2009) Basin scale alteration features and their implications for ore formation in the Paleoproterozoic Peräpohja schist belt, northwestern Finland. In: Smart science for exploration and mining: proceed 10th biennial SGA meet. Townsville, Australia, pp 457–459

Kyläkoski M, Hanski E, Huhma H (2012) The Petäjäskoski formation, a new lithostratigraphic unit in the Paleoproterozoic Peräpohja Belt, northern Finland. Bull Geol Soc Finl 84:85–120

Lahtinen R, Huhma H (2019) A revised geodynamic model for the Lapland-Kola orogen. Precambrian Res 330:1–19. https://doi.org/10.1016/j.precamres.2019.04.022

Lahtinen R, Korja A, Nironen M (2005) Palaeoproterozoic tectonic evolution of the Fennoscandian shield. In: Lehtinen M, Nurmi PA, Rämö OT (eds) Precambrian bedrock of Finland—key to the evolution of the Fennoscandian shield. Elsevier, Amsterdam, pp 418–532. https://doi.org/10.1016/S0166-2635(05)80012-X

Lahtinen R, Hallberg A, Korsakova M, Sandstad JS, Eilu P (2012) Main metallogenic events in Fennoscandia. Geol Surv Finl Spec Pap 53:397–401

Lahtinen R, Sayab M, Karell F (2015) Near-orthogonal deformation successions in the poly-deformed Paleoproterozoic Martimo Belt: implications for the tectonic evolution of northern Fennoscandia. Precambrian Res 270:22–38. https://doi.org/10.1016/j.precamres.2015.09.003

Lahtinen R, Huhma H, Sayab M, Lauri LS, Hölttä P (2018) Age and structural constraints on the tectonic evolution of the Palaeoproterozoic Central Lapland Granitoid complex in the Fennoscandian shield. Tectonophysics 745:305–325. https://doi.org/10.1016/j.tecto.2018.08.016

Lang JR, Baker T (2001) Intrusion-related gold systems: the present level of understanding. Mineral Deposita 36:477–489. https://doi.org/10.1007/s001260100184

Lehtonen M, Airo ML, Eilu P, Hanski E, Kortelainen V, Lanne E, Manninen T, Rastas P, Räsänen J, Virransalo P (1998) The stratigraphy, petrology and geochemistry of the Kittilä greenstone area, northern Finland: a report of the Lapland Volcanite Project. Geol Surv Finl Rep Invest 140 **(in Finnish with English summary)**

Mänttäri I (1995) Lead isotope characteristics of epigenetic gold mineralization in the Palaeoproterozoic Lapland greenstone belt, northern Finland. Geol Surv Finl Bull 381

McCuaig TC, Kerrich R (1998) P-T-t-deformation-fluid characteristics of lode gold deposits: evidence from alteration systematics. Ore Geol Rev 12:381–454. https://doi.org/10.1016/S0169-1368(98)80002-4

Mikucki EJ (1998) Hydrothermal transport and depositional processes in Archean lode-gold systems: a review. Ore Geol Rev 13:307–321. https://doi.org/10.1016/S0169-1368(97)00025-5

Mikucki EJ, Ridley JR (1993) The hydrothermal fluid of Archaean lode-gold deposits at different metamorphic grades: compositional constraints from ore and wallrock alteration assemblages. Mineral Deposita 28:461–481. https://doi.org/10.1007/BF02431603

Molnar F, O'Brien H, Lahaye Y, Kurhila M, Middleton A, Johanson B (2017) Multi-stage hydrothermal processes and diverse metal associations in orogenic gold deposits of the Central Lapland Greenstone Belt, Finland. In: Mineral Resources to Discover: Proceed 14th SGA Biennial Meet, Quebec City, Canada pp 63–66

Molnar F, Middleton A, Stein H, O'Brien H, Lahaye Y, Huhma H, Pakkanen L, Johanson B (2018) Repeated syn- and post-orogenic gold mineralization events between 1.92 and 1.76 Ga along the Kiistala Shear Zone in the Central Lapland Greenstone Belt, northern Finland. Ore Geol Rev 101:936–959. https://doi.org/10.1016/j.oregeorev.2018.08.015

Mutanen T, Huhma H (2001) U-Pb geochronology of the Koitelainen, Akanvaara and Keivitsa layered intrusions and related rocks. In: Vaasjoki M (ed.) Radiometric Age Determinations from Finnish Lapland and Their Bearing on the Timing of Precambrian Volcano-Sedimentary Sequences. Geol Surv Finl Spec Pap 33: 229–246

Neumayr P, Hagemann SG (2002) Hydrothermal fluid evolution within the Cadillac tectonic zone, Abitibi greenstone belt, Canada: relationship to auriferous fluids in adjacent second- and third-order shear zones. Econ Geol 97:1203–1225. https://doi.org/10.2113/gsecongeo.97.6.1203

Neumayr P, Hagemann SG, Couture JF (2000) Structural setting, textures, and timing of hydrothermal vein systems in the Val-d'Or camp, Abitibi, Canada: implications for the evolution of transcrustal, second- and third-order fault zones and gold mineralization. Can Jour Ear Sc 37:95−115. https://doi.org/10.1139/cjes-37-1-95

Niiranen T, Lahti I, Nykänen V, Karinen T (2014) Central Lapland Greenstone Belt 3D modeling project final report. Geol Surv Finl Rep Invest 209

Niiranen T, Lahti I, Nykänen V (2015) The orogenic gold potential of the Central Lapland greenstone belt, northern Fennoscandian shield. In: Maier WD, Lahtinen R, O'Brien H (eds) Mineral deposits of Finland. Elsevier, Amsterdam, pp 733–752. https://doi.org/10.1016/B978-0-12-410438-9.00028-5

Nironen M (2017) Structural interpretation of the Peräpohja and Kuusamo belts and Central Lapland, and a tectonic model for northern Finland. Geo Surv Finl Rep Invest 234

Pankka HS, Vanhanen EJ (1992) Early Proterozoic Au-Co-U mineralization in the Kuusamo district, northeastern Finland. Precambrian Res 58:387–400. https://doi.org/10.1016/0301-9268(92)90126-9

Patison NL (2007) Structural controls on gold mineralization in the Central Lapland Greenstone Belt. Geol Surv Finl Spec Pap 44: 105–122

Patison NL, Korja A, Lahtinen R, Ojala VJ (2006) FIRE seismic reflection profiles 4, 4A and 4B; insights into the crustal structure of northern Finland from Ranua to Näätämö. In: Kukkonen IT, Lahtinen, R (eds) Finnish Reflection Experiment FIRE 2001 −2005. Geol Surv Fin Spec Pap 43:161–222

Perttunen V, Vaasjoki M (2001) U-Pb geochronology of the Peräpohja schist belt, northwestern Finland. In: Vaasjoki, M (ed.) Radiometric Age Determinations from Finnish Lapland and Their Bearing on the Timing of Precambrian Volcano-Sedimentary Sequences. Geol Surv Finl Spec Pap 33:45–84

Petersen SB, Makovicky E, Li JL, Rose-Hansen J (1999) Mustard gold from the Dongping Au-Te deposit, Hebei Province, People's Republic of China. N J Miner M 8:337–357

Ranta JP, Molnar F, Hanski E, Cook N (2018) Epigenetic gold occurrence in a Paleoproterozoic meta-evaporitic sequence in the Rompas-Rajapalot au system, Peräpohja belt, northern Finland. Bull Geol Soc Finl 52:64–103

Rastas P, Huhma H, Hanski E, Lehtonen MI, Härkönen I, Kortelainen V, Mänttäri I, Paakkola J (2001) U–Pb isotopic studies on the Kittilä greenstone area, Central Lapland, Finland. In: Vaasjoki M (ed.) Radiometric Age Determinations from Finnish Lapland and Their Bearing on the Timing of Precambrian Volcano-Sedimentary Sequences. Geol Surv Finl Spec Pap 33:95–141

Riedel W (1929) Zur Mechanik geologischer Brucherscheinungen. Centralbl Min Geol Pal B, Stuttgart, pp 354–368

Rudnick R, Gao S (2003) Composition of the continental crust. Treatise Geochem 3:1–64. https://doi.org/10.1016/B0-08-043751-6/03016-4

Sayab M, Molnar F, Aerden D, Niiranen T, Kuva J, Välimaa J (2019) A succession of near-orthogonal horizontal tectonic shortenings in the Paleoproterozoic Central Lapland Greenstone Belt of Fennoscandia: constrains from the world-class Suurikuusikko gold deposit. Mineral Deposita. https://doi.org/10.1007/s00126-019-00910-7

Shackleton JM, Spry P, Bateman R (2003) Telluride mineralogy of the Golden Mile Deposit, Kalgoorlie, Western Australia. Can Min 41: 1503–1524. https://doi.org/10.2113/gscanmin.41.6.1503

Sibson RH, Robert F, Poulsen KH (1988) High-angle reverse faults, fluid-pressure cycling, and mesothermal gold-quartz deposits. Geol 16:551–555. https://doi.org/10.1130/0091-7613(1988)016<0551:HARFFP>2.3.CO;2

Slack JF (2012) Strata-bound Fe-Co-Cu-Au-Bi-Y-REE deposits of the Idaho cobalt belt: multistage hydrothermal mineralization in a magmatic-related iron oxide-copper-gold system. Econ Geol 107: 1089–1113. https://doi.org/10.2113/econgeo.107.6.1089

Slack JF, Causey JD, Eppinger RG, Gray JE, Johnson CA, Lund KI, Schulz KJ (2010-2012) (2010) Co-Cu-Au deposits in metasedimentary rocks. A preliminary report. U.S. Geol Surv Open-File Rep 13:1–19

Spence-Jones C, Jenkin G, Boyce A, Hill N, Sangster C (2018) Tellurium, magmatic fluids and orogenic gold: an early magmatic fluid pulse at Cononish gold deposit, Scotland. Ore Geol Rev 102: 894–905. https://doi.org/10.1016/j.oregeorev.2018.05.014

Stephens MB, Andersson J (2015) Migmatization related to mafic underplating and intra- or back-arc spreading above a subduction boundary in a 2.0–1.8 Ga accretionary orogen, Sweden. Precambrian Res 264:235–257. https://doi.org/10.1016/j.precamres.2015.04.019

Thompson RM (1949) The telluride minerals and their occurrence in Canada. Am Min 34:342–382

Thompson JHF, Sillitoe RH, Baker T, Lang JR, Mortensen JK (1999) Intrusion-related gold deposits associated with tungsten-tin provinces. Mineral Deposita 34:323–334. https://doi.org/10.1007/s001260050207

Väänänen J, Lehtonen MI (2001) U-Pb isotopic age determinations from the Kolari– Muonio area, western Finnish Lapland. In: Vaasjoki M (ed.) Radiometric Age Determinations from Finnish Lapland and Their Bearing on the Timing of Precambrian Volcano-Sedimentary sequences. Geol Surv Finl Spec Pap 33:85–93

Väisänen M (2002) Structural features in the Central Lapland Greenstone Belt, northern Finland. Geol Surv Finl K21:42

Vanhanen E (2001) Geology, mineralogy and geochemistry of the Fe-Co-Au-(U) deposits in the Paleoproterozoic Kuusamo Schist Belt, northeastern Finland. Geol Surv Finl Bull 399

Ward P, Härkönen I, Nurmi PA, Pankka HS (1989) Structural studies in the Lapland greenstone belt, northern Finland and their application to gold mineralization. Geol Surv Finl Spec Pap 10

Wyche NL, Eilu P, Koppström K, Kortelainen VJ, Niiranen T, Välimaa J (2015) The Suurikuusikko gold deposit (Kittilä mine), northern Finland. In: Maier WD, Lahtinen R, O'Brien H (eds) Mineral deposits of Finland. Elsevier, Amsterdam, pp 411–434. https://doi.org/10.1016/B978-0-12-410438-9.00016-9

Yardley BWD, Cleverley JS (2013) The role of metamorphic fluids in the formation of ore deposits. Geol Soc London Spec Publ 393:117–134. https://doi.org/10.1144/SP393.5

Yardley BWD, Graham JT (2002) The origins of salinity in metamorphic fluids. Geofluids 2:249–256. https://doi.org/10.1046/j.1468-8123.2002.00042.x

Zhao J, Brugger J, Grundler P, Xia F, Chen G, Pring A (2009) Mechanism and kinetics of a mineral transformation under hydrothermal conditions: Calaverite to metallic gold. Am Min 94:1541–1555. https://doi.org/10.2138/am.2009.3252